Published in final edited form as:
J Comp Neurol. 2005 March 21; 483(4): 458–475.

Quantitative Changes in Calretinin Immunostaining in the Cochlear Nuclei after Unilateral Cochlear Removal in Young Ferrets

Verónica Fuentes-Santamaria*, **Juan Carlos Alvarado**, **Anna R. Taylor**, **Judy K. Brunso-Bechtold**, and **Craig K. Henkel**
Department of Neurobiology and Anatomy, Wake Forest University School of Medicine, Winston–Salem, North Carolina 27157-1010

Abstract

Neurons of the cochlear nuclei receive axosomatic endings from primary afferent fibers from the cochlea and have projections that diverge to form parallel ascending auditory pathways. These cells are characterized by neurochemical phenotypes such as levels of calretinin. To test whether or not early deafferentation results in changes in calretinin immunostaining in the cochlear nucleus, unilateral cochlear ablations were performed in ferrets soon after hearing onset (postnatal day [P] 30–P40). Two months later, changes in calretinin immunostaining as well as cell size, volume, and synaptophysin immunostaining were assessed in the anteroventral (AVCN), posteroventral (PVCN), and dorsal cochlear nucleus (DCN). A decrease in calretinin immunostaining was evident ipsilaterally within the AVCN and PVCN but not in the DCN. Further analysis revealed a decrease both in the calretinin-immunostained neuropil and in the calretinin-immunostained area within AVCN and PVCN neurons. These declines were accompanied by significant ipsilateral decreases in volume as well as neuron area in the AVCN and PVCN compared with the contralateral cochlear nucleus and unoperated animals, but not compared with the DCN. In addition, there was a significant contralateral increase in calretinin-immunostained area within AVCN and PVCN neurons compared with control animals. Finally, a decrease in area of synaptophysin immunostaining in both the ipsilateral AVCN and PVCN without changes in the number of boutons was found. The present data demonstrate that unilateral cochlear ablation leads to 1) decreased immunostaining of the neuropil in the AVCN and PVCN ipsilaterally, 2) decreased calretinin immunostaining within AVCN and PVCN neurons ipsilaterally, 3) synaptogenesis in the AVCN and PVCN ipsilaterally, and 4) increased calretinin immunostaining within AVCN and PVCN neurons contralaterally.

Keywords

calcium-binding protein; deafferentation; inferior colliculus; synaptogenesis; neural plasticity; image analysis

Morphologically distinct axosomatic endings of primary afferent fibers from the cochlea distribute differentially to specific cell types within the cochlear nuclei (e.g., Osen, 1969;Kane, 1973,1974;Ryugo and Parks, 2003). In turn, each cell type in the cochlear nuclei projects to higher auditory centers, forming parallel ascending pathways that process different features of sound (for review, see Cant and Benson, 2003). Most of these ascending auditory pathways end in an orderly tonotopic array of fibrodendritic layers in the central nucleus of the inferior colliculus (IC) (Brunso-Bechtold et al., 1981;Oliver and Morest, 1984;Druga and Sika,

*Correspondence to: Verónica Fuentes-Santamaria, Department of Neurobiology and Anatomy, Wake Forest University School of Medicine, Medical Center Boulevard, Winston-Salem, NC 27157-1010. E-mail: vfuentes@fubmc.edu.

1984;Shneiderman and Henkel, 1987). Experience-dependent changes in these pathways presumably comprise the structural corollary of functional plasticity and permit adaptive changes in auditory processing. Loss of cochlear integrity has been shown to result in a variety of morphological, biochemical, and metabolic changes throughout the auditory brainstem (Sie and Rubel, 1992;Potashner et al, 1997;Illing et al., 2000;Tucci et al., 2001;Syka, 2002). After deprivation of presynaptic activity, an efficient regulation of intracellular calcium within neurons is crucial for neuronal function and synaptic plasticity (Ghosh and Greenberg, 1995). One of the neuronal mechanisms that contribute to calcium homeostasis is a family of intracellular proteins known as calcium-binding proteins (Baimbridge et al., 1992).

Calcium-binding proteins are expressed abundantly and are distributed in morphologically distinct cells and fibers in nuclei of the auditory system (Caicedo et al., 1997,Kubke et al., 1999;Idrizbegovic et al., 2001). The role of these proteins in calcium-dependent mechanisms during development (Lohmann and Friauf, 1996;Henkel and Brunso-Bechtold, 1998;Kubke et al., 1999) and neural processing (Zettel et al., 1991;Vater and Braun, 1994;Frisina et al., 1995,Caicedo et al., 1996;Korada and Schwartz, 2000) and in response to deafferentation (Winsky and Jacobowitz, 1995;Caicedo et al., 1997;Parks et al., 1997;Förster and Illing, 2000,Stack and Code, 2000;Alvarado et al., 2004;Fuentes-Santamaria et al., 2003a,2003b) has been studied in many sensory systems and species but is still poorly understood (Arai et al., 1991;Lim and Brunjes, 1999;Philpot et al., 1997). One of these proteins, calretinin, is localized in a subset of auditory neurons that are linked to a specific time-coding pathway to the IC and appears to play a role in the control of calcium homeostasis by buffering the calcium that enters cells during synaptic activation (Baimbridge et al., 1992;Andressen et al., 1993;Miller, 1995). Nevertheless, the precise role of calretinin in modulating the calcium-mediated effects on neuronal activity and synaptic plasticity is still unclear.

Calretinin-immunoreactive fibers in the IC form a dense plexus of branches and endings that distribute parallel to the fibrodendritic layers of the central nucleus of the IC (Fuentes-Santamaria et al., 2003a). This plexus is likely to arise from one or more cell types in the cochlear nuclei, superior olivary complex, or nuclei of the lateral lemniscus that also contain calretinin (Alvarado et al., 2004;Fuentes-Santamaria et al., 2003b). Recently, we demonstrated that cochlear ablation after hearing onset leads to an increase in this calretinin-immunostained plexus in the contralateral IC (Fuentes-Santamaria et al., 2003a). Moreover, calretinin is downregulated within the neuropil of the medial superior olivary nucleus (MSO) bilaterally and the lateral superior olivary nucleus (LSO) ipsilaterally (Alvarado et al., 2004). Because upregulation and/or downregulation of calcium-binding protein in axons and their endings may reflect changes in a subset of cell types that project to these targets (Winsky and Jacobowitz, 1995;Caicedo et al., 1997), we were interested in correlating changes in the calretinin immunostaining in the IC (Fuentes-Santamaria et al., 2003a) with that in a presumed brainstem source of these projections, the cochlear nucleus. (Unpublished observations from our laboratory indicate that after injections of biotinylated dextran amine [BDA] in the inferior colliculus, multipolar cells are retrogradely labeled in the cochlear nucleus that are also calretinin immunostained.)

The cochlear nucleus complex is a large brainstem structure that comprises a group of nuclei, the anterior and posteroventral cochlear nuclei and the dorsal cochlear nucleus, each containing different populations of neurons (Cant, 1992). These neurons are innervated by primary auditory fibers from spiral ganglion neurons, which bifurcate in an ascending branch to the anterior ventral cochlear nucleus and a descending branch to the posterior ventral and dorsal cochlear nuclei (Ryugo, 1992). After branching, each primary fiber from the cochlea synapses with the main cell types in the cochlear nucleus, bushy cells, octopus cells, multipolar cells, and stellate cells (Osen, 1969). Each of these cells gives rise to functionally different ascending

systems that converge in the inferior colliculus (Adams, 1979;Cant, 1982;Ryugo and Willard, 1985).

The present study examined the effects of unilateral cochlear ablation after hearing onset on the expression of calretinin in the cochlear nuclei of young adult ferrets. The following questions were addressed: 1) are there changes in the level of calretinin in cochlear nucleus neurons and fibers following cochlear ablation? 2) how do changes in calretinin immunostaining relate to overall morphometric changes in the cochlear nucleus following cochlear ablation? and 3) how do changes in calretinin-immunostained neuropil correspond to changes in synaptic endings labeled for synaptophysin in the cochlear nucleus following cochlear ablation? The relation of changes in calretinin immunostaining in cochlear nucleus neurons to upregulation or downregulation of calretinin in endings in IC following cochlear ablation is discussed. Preliminary results have been published in abstract form (Fuentes-Santamaria et al., 2003b).

MATERIALS AND METHODS

Animals and cochlear surgery

To determine whether early hearing loss results in changes in calretinin immunostaining in the cochlear nuclei that could alter calretinin immunostaining in the IC, unilateral cochlear ablations were performed soon after hearing onset in 30–40 postnatal-day-old (P30–P40) ferrets. Data were obtained from 11 animals. Experimental animals (N = 8) were anesthetized with a combination of ketamine (30 mg/kg) and xylazine (5 mg/kg) delivered intramuscularly. Surgical procedures have been described previously (Fuentes-Santamaria et al., 2003a). Briefly, under aseptic conditions, the cochlea was exposed through the right bulla and removed with forceps, and the remaining cochlear contents were aspirated by using a Pasteur pipette attached to a vacuum. After the skin was sutured, animals were returned to their cages and maintained with free access to food and water for the appropriate survival time. Microscopic inspection of the dissected bulla was performed in order to assess the extent of the cochlear ablation. Age-matched unlesioned animals served as controls (N = 3). All animal protocols conformed to National Institutes of Health standards and were approved by the institution's Animal Care and Use Committee.

Calretinin and synaptophysin immunohistochemistry

After a postsurgical survival time of 50–70 days, ferrets were deeply anesthetized with an intramuscular overdose of ketamine (50 mg/kg) and xylazine (5 mg/kg) and perfused transcardially with 0.1% sodium nitrite in 0.1 M phosphate buffer, pH 7.4, followed by fixative (4% paraformaldehyde and 0.1% glutaraldehyde in 0.1 M phosphate buffer, pH 7.4). The brains were then blocked in situ, removed from the cranium, and immersed in the same fixative for 3 hours at room temperature; for cryo-protection, they were immersed overnight in 30% sucrose at 4°C. Serial, coronal sections (50 μm) were cut on a sliding microtome and placed in 0.1 M phosphate buffer (pH 7.4). Free-floating sections were incubated overnight at 4°C in mouse anti-calretinin monoclonal antibody (1: 1,500; MAB1568, lot no. 23090043, Chemicon, Temecula CA) or mouse anti-synaptophysin monoclonal antibody (1:2,000; MAB5258, lot no. 22040974, Chemicon). The tissue then was washed and incubated in a 1:200 dilution of biotinylated secondary antibody (Vector, Burlingame, CA) for two hours at room temperature. The Vector avidin-biotin procedure (Hsu et al., 1981) was used to link the antigen-antibody complex to horseradish peroxidase (HRP), which was then visualized with diaminobenzidine histochemistry. Finally, the sections were washed thoroughly, mounted on gelatin-coated slides, air-dried, dehydrated in ethanol, cleared in xylene, and coverslipped with cytoseal (Stephens Scientific, Camden, NJ). Adjacent sections were stained with cresyl violet.

Immunohistochemical controls

Omission of primary antibody—Control sections were incubated in the absence of primary antibodies; no immunostaining was detected under these conditions. The specificity of these particular antibodies has been shown for various cell types in a variety of brain regions (calretinin: Couper Leo et al., 2000;Di Cunto et al., 2000;Dyer and Cepko, 2000;Korada et al., 2000;Nunzi et al., 2001;O'Donnell et al., 2001;Coutts et al., 2002;Mirich et al., 2002;Fuentes-Santamaria et al., 2003a;Alvarado et al., 2004;Lee et al., 2004; synaptophysin: Kawai and Senba, 2000; Hu et al., 2001; Masliah et al., 2001;Csaba et al., 2002;Kawasaki et al., 2003;Khan et al., 2003).

Western blot—The specificity of the antibodies was tested by Western blot analysis. Fresh tissue dissected from the cochlear nucleus was collected from a P49 ferret and homogenized and sonicated in lysis buffer containing 50 mM Tris, 150 mM NaCl, 1 mM EDTA, 1 mM EGTA, 1% NP-40, 1 μg/ml leupeptin, 1 μg/ml aprotinin, and 1 mM phenylmethylsulfonyl fluoride (PMSF) at pH 7.4. The cell extracts were then cleared by centrifugation at 14,000 rpm, and protein concentration was determined by a modified Lowry assay (Bio-Rad, Hercules, CA). Then 10 μg of protein was loaded onto a 10% sodium dodecyl sulfate-polyacrylamide gel electrophoresis (SDS-PAGE) gel. Samples were separated and transferred to an Immobilin-P membrane (Millipore, Bedford, MA). Membranes were blocked with 5% nonfat dry milk in Tris-buffered saline plus 1% Tween-20 (blocking buffer) for 1 hour. The blot was incubated overnight at 4°C in a solution containing the primary antibodies to calretinin (1:1,000; MAB1568, Chemicon) and synaptophysin (1:1,000; MAB5258, Chemicon). Membranes were rinsed, incubated with an HRP-conjugated secondary antibody (1:5,000; Jackson ImmunoResearch, West Grove, PA) for 30 minutes, and detected by electrochemiluminescence (Pierce, Rockford, IL).

Measurements of cochlear nucleus volume

In order to measure the cochlear nucleus volume, dorsal and ventral subdivisions were defined according to Osen (1969) and Moore (1988). Using Neurolucida software (Microbrightfield, Colchester, VT), the perimeters of the anterior ventral cochlear nucleus (AVCN), posterior ventral cochlear nucleus (PVCN), and dorsal cochlear nucleus (DCN) were traced from cresyl violet sections throughout the rostrocaudal extent of each nucleus. The total volume of each nucleus in experimental and control groups was estimated from the compiled data using the Neuroexplorer component of Neurolucida.

Measurements of cross-sectional area of cochlear nucleus neurons

Cross-sectional area of AVCN, PVCN, and DCN neurons in both normal and ablated animals was measured in five equally spaced cresyl violet sections from the middle third of each cochlear nucleus using Neuroexplorer and Neurolucida software. Using a 50× objective, three fields were sampled randomly in each subdivision, and only neurons with a well-defined cytoplasm, nuclear outline, and nucleolus were measured (Mostafapour et al., 2000). The criteria for the classification of cochlear nucleus neurons in the ferret were based on cell morphology and location within the nucleus (Osen, 1969;Floris et al., 1994;Doucet and Ryugo, 1997). In the dorsal cochlear nucleus, *pyramidal cells* were located in the granular cell layer and identified by their relatively large and bipolar cell bodies, which usually taper and give rise to one or two dendrites. The *giant cells* were the largest cell type in the cochlear nucleus, with a relatively large nucleus and dendrites emerging from the cell body in all directions. These cells were located in the central region of the dorsal cochlear nucleus. *Unipolar brush cells* were located in the granular cell layer and were identified by a single thick dendrite of varying length terminating in a brush-like tip with several short branches (Floris et al., 1994;Doucet and Ryugo, 1997). *Granular cells*, the smallest cells in the cochlear nucleus and

similar to pyramidal cells, were distributed in the granular cell domain. The granular cells constituted a continuous layer covering the surface of the cochlear nucleus, giving rise to two to four primary dendrites of varying lengths. In the ventral cochlear nucleus, *octopus cells* were identified by the characteristic of their dendrites, which give the cells an octopus-like appearance. These cells had a centrally located nucleus and dendrites that crossed a great number of descending cochlear branches. *Globular cells* were easily identified based on the eccentricity of the nucleus, the oval to round shape of the cell body, and a location within the cochlear nerve root. *Multipolar cells* had a centrally located nucleus and three or more visible dendrites. These cells were distributed throughout the central region of the central cochlear nucleus. *Spherical cells* were round, with a centrally located nucleus, and were found mainly in the lateral and rostral part of the ventral cochlear nucleus.

Densitometric analyses of calretinin and synaptophysin immunostaining

Sections were examined with brightfield illumination by using a Nikon Optiphot research photomicroscope with a 20× objective (calretinin-immunostained sections) or a 50× oil immersion objective (synaptophysin-immunostained sections). Images were captured with a Spot CCD color video camera, model RT Slider (Diagnostic Instruments, Sterling Heights, MI) attached to the microscope. The densitometric analysis method used in this experiment has been described in detail previously (Fuentes-Santamaria et al., 2003a;Alvarado et al., 2004).

Analysis of calretinin immunostaining was performed in six equally spaced sections extending throughout the rostrocaudal dimension of each nucleus. To compare across cases, measurements of the *mean gray level* in the AVCN, PVCN, and DCN were normalized, and threshold detection was set 1 standard deviation above the value of the medial longitudinal fasciculus, a neutral structure visible in all the sections and unrelated to any direct or indirect auditory pathways. Because immunostaining can be used as a relative measure of antigen concentration (Huang et al., 1996; Yao and Godfrey, 1997; Lin and Talman, 2000), the *mean gray level* within the AVCN, PVCN, and DCN was used as an indirect indicator of the amount of calretinin in each nucleus.

Accordingly, all mean gray levels were corrected by dividing the averaged values on each side of the brain by the averaged value from the medial longitudinal fasciculus on the same side (Fuentes-Santamaria et al., 2003; Alvarado et al., 2004). This measure provides a general estimation regarding the effect of cochlear ablation on calretinin immunostaining throughout the nucleus. Because any changes in the overall levels of immunostaining within the cochlear nucleus could be caused by changes in immunostained neuropil or neurons, both the *mean gray level* within neurons and the *neuron immunostained area* or mean cross-sectional area of calretinin immunoreactivity within individual neurons were measured (Alvarado et al., 2004). Thus, in calretinin-immunoreacted sections, three indices were measured: 1) the *mean gray level within each nucleus*, 2) the *mean gray level within neurons*, and 3) the *immunostained area within neurons*.

Synaptophysin immunostaining was analyzed in four equally spaced sections from the middle third of each subdivision of the cochlear nucleus. In each section, using a50× oil immersion objective, three fields (2.72×10^4 μm^2 per field) were sampled at random points in each subdivision, avoiding the cochlear nerve root and the borders of the subdivision (Fig. 1). After normalization, the threshold was set 2 standard deviations above the value of the field. Objects exceeding the threshold were identified as labeled, and the *mean gray level of synaptophysin immunostaining*, the *synaptophysin-immunostained area*, and the *mean number of immunostained boutons* were measured as described previously (Fuentes-Santamaria, 2003a;Alvarado et al., 2004). The mean gray level of synaptophysin immunostaining was used as an indirect indicator of synaptophysin level (Masliah et al., 1990,1991;Davies et al.,

1998;Stroemer et al., 1998;Kadish et al., 2002;Kadish and van Groen, 2002;Li et al., 2002;Kadish and van Groen, 2003), and the immunostained area was used to estimate the area occupied by synaptic endings (Benson et al., 1997;Fuentes-Santamaria et al., 2003a). The immunostained area was calculated as the summed area of all labeled pixels in the field and was expressed as the percentage of the entire field. The mean number of boutons was used to evaluate the possibility of increases or decreases in synaptic input to the cochlear nucleus (Benson et al., 1997;Fuentes-Santamaria et al., 2003a;Alvarado et al., 2004). In order to measure the number of synaptic endings in each field, puncta between 0.46 μm^2 and 84 μm^2 were counted in this analysis so as to include both smaller puncta in the neuropil and larger, combined profiles of several puncta surrounding neurons (perisomatic profiles).

Because volume changes affect both the measured synaptophysin-immunostained area and the density of boutons, a shrinkage factor was calculated by dividing the mean volume of each subdivision in experimental animals by that from control animals; then the synaptophysin-immunostained area and number of synaptic endings values were multiplied by the shrinkage factor (Benson et al., 1997;Muly et al., 2002). In the results, values will be referred to as not corrected (the shrinkage factor correction was not applied) or corrected (the shrinkage factor correction was applied).

Image processing

To prepare the figures shown here, the size and brightness of the images were adjusted by using Adobe Photoshop (version 5.5) and Canvas (version 6.0). These adjustments in no way altered the immunostaining pattern of each antibody.

Statistical analysis

All data were expressed as mean ± SD and were analyzed statistically by using Student's t-test. Statistical significance was determined at a level of $P < 0.05$.

RESULTS

Western blot analyses of calretinin and synaptophysin in the cochlear nucleus

The specificity of calretinin and synaptophysin antibodies was assessed with a Western blot analysis of membrane fractions from the ferret cochlear nucleus (Fig. 2). These antibodies gave rise to a single band with an estimated molecular weight of 31 kDa for calretinin and 38 kDa for synaptophysin.

General observations

The cochlear nuclei in the ferret have been described previously (Moore, 1988). The distribution and morphology of AVCN and PVCN neurons are similar to those in the cat (Osen, 1969), with multipolar, globular, and spherical cells in the AVCN and multipolar, globular, and octopus cells in the PVCN. The DCN does not have a prominent laminar organization, although three layers can be recognized: a *molecular layer* with scattered small cells and granular cells and fibers; a *granular cell layer* with fusiform cells, cartwheel cells, granule cells, and unipolar brush cells; and a *central region of the DCN* with small and giant cells (Moore, 1988). In the present study, the patterns of calretinin immunostaining will be described first, in the cochlear nuclei of the normal age-matched control animals. For comparison with the cochlear ablation cases, three quantitative indices of calretinin immunostaining were evaluated: 1) the *mean gray level of calretinin within the nucleus*, 2) the *mean gray level within neurons*, and 3) the *neuron immunostained area*. Second, for quantification of synaptophysin immunostaining, three indices were also measured: 1) the *mean gray level*, 2) the

immunostained area, and 3) the *mean number of immunolabeled boutons* (see Materials and Methods).

Calretinin distribution in control cases

Ventral cochlear nucleus—A densely immunostained neuropil was evident throughout the rostrocaudal extent of the AVCN (insert in Fig. 3A) and PVCN (Fig. 4C). In addition, spherical (Fig. 5A,B), globular (Fig. 5C), and multipolar (Fig. 5D) neurons in the AVCN and octopus (Fig. 5E), globular (Fig. 5F,G), and multipolar (Fig. 5H) cells in the PVCN were calretinin immunostained. Although most of the cells were immunopositive for calretinin qualitatively, a few unstained cells were also observed, presumably corresponding to spherical cells, globular cells, and multipolar cells, because these cells received immunostained calyciform endings. As expected in control cases, no differences between the left and right sides of either the AVCN or PVCN were observed in the overall mean gray level of calretinin immunostaining (compare Fig. 3A with B and Fig. 4A with B), in the mean gray level, or in the calretinin-immunostained area within AVCN or PVCN neurons (Table 1).

Dorsal cochlear nucleus—Calretinin immunostaining was detected mainly within somata in the granular cell layer (*grcl* in Fig. 4D). In contrast, immunostained cells only rarely were seen in the molecular layer (*ml* in Fig. 4D) and central region (*crdcn* in Fig. 4D) of the DCN. The immunostained somata in the granule cell layer were mostly small to intermediate in size and were round or oval in shape, suggesting that they were granule cells (Fig. 5I,J). Labeled cells with single, thick dendrites of varying length and terminating in a brush-like tip with several short branches resembled unipolar brush cells (Fig. 5K,L; Floris et al., 1994,Doucet and Ryugo, 1997;Idrizbegobic et al., 2001). Compared with the ventral subdivisions in which most of the neuronal types were calretinin immunostained, only a few cell types were immunostained in the dorsal subdivision. The neuropil in the DCN was immunostained lightly, and in some cases the immunostaining was distributed in patches, especially in the granule cell layer (Fig. 4D). The relatively low level of immunostaining in the DCN neuropil is contrasted quantitatively in Table 1 with higher mean gray levels present in the AVCN and PVCN. Although the mean gray level within neurons in each subdivision was similar, the immunostained area within neurons in the DCN was smaller than in the AVCN and PVCN, reflecting the smaller cell types that are labeled in the DCN compared with the other subdivision. No differences between the left and right sides were observed in either the mean gray level of calretinin immunostaining throughout the nucleus or in the calretinin-immunostained area and mean gray level within DCN neurons (Table 1).

Calretinin distribution in cochlear ablation cases

Ventral cochlear nucleus—Following unilateral cochlear ablation, the overall mean gray level of calretinin immunostaining decreased significantly in the ipsilateral AVCN ($P < 0.01$) and PVCN ($P < 0.01$) compared with the contralateral side (compare insert in Fig. 3D with insert in Fig. 3C, for AVCN and Fig. 6D with C, for PVCN) and with control animals (compare insert in Fig. 3D with insert in Fig. 3A, for AVCN and Fig. 6D with Fig. 4C, for PVCN; also see Table 1). In addition, the neuron immunostained area decreased significantly in the ipsilateral AVCN (14.36%; P< 0.01) and PVCN (14.82%; $P < 0.01$) and increased in the contralateral AVCN (7.71%; $P < 0.01$) and PVCN (7.65%; $P < 0.01$) compared with unoperated animals. Because no changes in the neuron mean gray level were found between experimental and control ferrets (Table 1), the decrease in the overall mean gray level of calretinin immunostaining might be due to a decreased immunostaining in the neuropil.

Dorsal cochlear nucleus—In all eight cases with unilateral cochlear ablation, the DCN in ablated animals did not show a different immunostaining pattern compared with unoperated ferrets (compare Fig. 6A,B with Fig. 4A,B). Quantitative measurements of the mean gray level

of calretinin immunostaining in the DCN and the neuron immunostained area of calretinin and mean gray level within the DCN neurons did not reveal significant differences either between sides or between experimental and control cases (compare Fig. 6F with E and 4D; also see Table 1).

Comparison of cochlear nucleus volume in control and ablated cases

Cochlear ablation resulted in an obvious ipsilateral decrease in overall size of both the AVCN (compare Fig. 3D with C and A) and the PVCN (compare Fig. 6B with A and Fig. 4A), but not in the DCN, compared with the contralateral side and control animals. To quantify this decrease, AVCN, PVCN, and DCN volumes on both sides were measured in control and ablated animals. A significant reduction in AVCN (Fig. 7A) and PVCN (Fig. 7B) volumes was evident on the side of the lesion compared with both the contralateral side ($P < 0.05$) and control animals ($P < 0.05$). The reductions in volume of the ipsilateral side relative to control animals were 33% for the AVCN and 23% for the PVCN.

Comparison of cross-sectional area of cresyl violet-stained neurons in the PVCN and AVCN in control and cochlear ablation cases

The reduction in calretinin-immunostained area within VCN neurons ipsilaterally could be due to cell shrinkage after deafferentation. To account for this possibility, neuron area was measured in adjacent cresyl violet-stained sections in control and cochlear ablation cases. A statistically significant decrease in the neuron area in the AVCN (11.58 %) and PVCN (11.79 %) was found on the ipsilateral side compared with control animals ($P < 0.05$), but there were no significant differences between neurons in the contralateral side and control animals in any of these nuclei. Considering that the percentage of cell shrinkage in the ipsilateral ventral cochlear nucleus was smaller than the percentage of reduction in the calretinin-immunostained area in ablated animals, the reduction in the immunostained area of calretinin could not be explained only by cell shrinkage, but instead suggests a decrease in the area of calretinin immunoreactivity within those neurons. In contrast, the significant increase in the calretininimmunostained area in the AVCN and PVCN on the contralateral side without changes in cell area, compared with unoperated animals, suggests an increase in the area occupied by calretinin within these cells. These findings indicate compensatory changes in calretinin among neurons in both cochlear nuclei.

Synaptophysin immunostaining in the cochlear nuclei

The reduction in the mean gray level of calretinin immunostaining throughout AVCN and PVCN described above could be due largely or in part to decreases in number of synaptic endings after deafferentation. To address this possibility, synaptophysin immunohistochemistry was used to evaluate overall changes in distribution of synaptic endings within each nucleus after cochlear ablation. The overall mean gray level, immunostained area, and number of synaptophysin immunostained boutons were measured in nine fields along the tonotopic axis of the AVCN, PVCN, and DCN (see Materials and Methods).

Ventral cochlear nucleus—In control ferrets, synaptophysin-immunostained endings were found in the neuropil (arrowheads in Figs. 8 and 9) and surrounding cochlear nucleus neurons (perisomatic profiles, arrows in Figs. 8 and 9) in both the AVCN and PVCN. In experimental ferrets, densitometric analysis of synaptophysin immunostaining in the AVCN and PVCN revealed no changes either between the ipsilateral and contralateral sides (AVCN or PVCN) or between either side and control ferrets for the mean gray level of synaptophysin immunostaining (Table 2). When the values were not corrected for tissue shrinkage, there were significantly more synaptophysin-immunostained boutons ipsilaterally in the AVCN ($P < 0.05$; Table 2) and PVCN ($P < 0.05$; Table 2) without changes in the immunostained area in ablated

ferrets compared with control animals. However, when these values were corrected for shrinkage of the nuclei, no change in the mean number of boutons was found compared with the contralateral side or to control ferrets, but there was a decrease in synaptophysin-immunostained area in the ipsilateral AVCN ($P < 0.05$; Table 2, corrected values for tissue shrinkage) and PVCN ($P < 0.05$; Table 2, corrected values for tissue shrinkage).

Dorsal cochlear nucleus—Synaptophysin immunostaining in the DCN appeared most frequently as punctate deposits (arrowheads in Fig. 10) in the neuropil and less frequently as larger profiles surrounding unstained cell bodies (arrows in Fig. 10) in both control (Fig. 10A,B) and ablated (Fig. 10C,D) animals. Analysis of the synaptophysin immunostaining in cochlear ablation cases revealed no changes either between the ipsilateral and the contralateral sides or between either side and control animals for the mean gray level of synaptophysin immunostaining, synaptophysin-immunostained area, or number of boutons (Table 2).

DISCUSSION

Analysis of calretinin immunostaining revealed a significant decrease in the immunostained neuropil in the ipsilateral AVCN and PVCN but not in the DCN after unilateral cochlear ablation. This decline was accompanied by a decrease in the mean cross-sectional area of cresyl violet-stained neurons in the ipsilateral AVCN and PVCN as well as a decrease in the volume of these subdivision. Considering that the percent reduction in cell size was slightly smaller than the percent reduction in neuron immunostained area of calretinin, the decreased immunostained area within AVCN and PVCN neurons might be in part, but not completely, attributed to cell shrinkage. Therefore, these data also suggest a small downregulation of calretinin within these neurons. Furthermore, downregulation of calretinin in the neuropil in the ipsilateral AVCN and PVCN was accompanied by a decrease in the synaptophysin-immunostained area without changes in number of endings, a scenario that might occur with a new growth of small synaptic endings after cochlear ablation. In addition to these changes, there was a small but significant increase in the calretinin-immunostained area within contralateral AVCN and PVCN neurons with no indication of a corresponding increase in cell size, suggesting an activity-dependent compensation in a subset of neurons that contribute to the calretinin-immunostained plexus in the central nucleus of the IC.

Technical considerations

The medial longitudinal fasciculus as a structure to set the threshold—The medial longitudinal fasciculus was selected as an internal standard to set an objective and consistent threshold for calretinin-immunostained structures because it was immunostained heavily by calretinin antibodies, had well-defined borders, and was unaffected by cochlear ablation. Any effect on staining of the medial longitudinal fasciculus by possible vestibular damage concomitant with cochlear ablation was assessed carefully on each side of the brain to avoid bias in analysis and interpretation of the data. In all cases analyzed, there was never a statistically significant difference in staining density in the medial longitudinal fasciculus between the left and right sides.

Relation of quantitative measurements of calretinin immunostaining to intracellular levels of calretinin—A basic assumption in interpreting the quantitative findings in this study is that increases or decreases in intracellular levels of the antigen, calretinin, will be reflected in matching changes in the magnitude of immunostaining, whether that is changes in area of the cytoplasm above threshold or the mean gray level of immunostaining. Although it has been established that the magnitude of immunostaining does not reflect absolute levels of the antigen (Davenport et al., 1990;Peretti-Renucci et al., 1991;Correa et al., 1991)—that is, a twofold change in antigen concentration does not

necessarily result in a twofold change in area or intensity of immunostaining—it has been demonstrated that the direction of change and the relative amount of change between different structures is a reliable indication of relative differences in levels of the antigen (Huang et al., 1996; Yao and Godfrey, 1997; Lin and Talman, 2000).

Calretinin immunostaining in the cochlear nuclei

Calretinin immunostaining is present in fibers and specific cell types in the ferret cochlear nuclei that, based on location, size, and shape, appear to include globular, spherical, and multipolar cells in the AVCN, multipolar and octopus cells in the PVCN, and unipolar brush cells and granular cells in the DCN. The pattern of calretinin immunostaining in cochlear nuclei has been well characterized in rat (Resibois and Roger, 1992;Lohmann and Friauf, 1996), mouse (Idrizvegovic et al., 2001), guinea pig (Winsky and Jacobowitz, 1995;Caicedo et al., 1997), bat (Vater and Braun, 1994), gerbil (Korada et al., 2000), and chick (Rogers, 1989). Similar to the present findings, all of these studies have reported that most calretinin-immunostained cells are localized in the ventral cochlear nucleus with only a few neuron types labeled in the DCN. One exception is the gerbil, in which some faintly calretinin-immunopositive cells were found in the deep layers of the DCN and in the PVCN (Korada et al., 2000). Also, a small population of DCN cells in rat, guinea pig, horseshoe bat, and mouse contain both the calretinin protein as shown by using immunohistochemistry (e.g., Arai et al., 1991;Idrizvegobic et al., 2001) and the calretinin mRNA as shown by using in situ hybridization (Winsky and Jacobowitz, 1995).

Effects of cochlear ablation on calretinin immunostaining in the cochlear nuclei

Cochlear ablation has been shown to produce different effects on calretinin immunostaining depending on the species, age at which deafferentation occurs, and survival time after cochlear ablation. Cochlear ablation in embryonic, hatchling, and adult birds at survival times from 3 hours to 7 days resulted in no changes in calretinin mRNA and immunostaining within cochlear nucleus neurons ipsilaterally (Parks et al., 1997;Stack and Code, 2000). In young adult guinea pigs, an increase was shown in calretinin immunostaining and calretinin mRNA in AVCN neurons 1 day after cochlear ablation, along with a persistent decrease in immunostaining in PVCN neurons (Winsky and Jacobowitz, 1995). In the same study, calretinin-immunostained neuropil in the AVCN, PVCN, and DCN was decreased at both 7 and 56 days post lesion. Similar to these findings, a subsequent study in adult guinea pig (Caicedo et al., 1997) reported reduced calretinin-immunostained neuropil as well as reduced calretinin immunostaining within neurons in both the AVCN and PVCN several hours after temporary sensory deprivation. The present findings corroborate the decrease in calretinin-immunostained neuropil in the deafferented AVCN and PVCN, although no changes were found in the mean gray level within AVCN and PVCN neurons. In addition, the present results demonstrated a decrease in the immunostained area ipsilaterally and an increase contralaterally within AVCN and PVCN neurons. It is likely that the differences in the mean gray level within neurons between this study and that of Caicedo et al. (1997) are due to a combination of factors such as age and type of deprivation, quantitative approaches, survival times, or species.

Correlation of activity in cochlear nuclei after cochlear ablation and calretinin immunostaining

Both decrease and increase of calretinin immunostaining may reflect changes in the levels of activity in the cochlear nuclei following cochlear ablation and concomitant changes in levels of intracellular calcium. Tucci et al. (2001) reported a decrease in cytochrome oxidase activity in the ipsilateral AVCN and an increase in the contralateral AVCN 48 hours after conductive hearing loss in young adult gerbils, suggesting a downregulation in activity in neurons in the deafferented side due to a loss of primary afferents (Luo et al., 1999;Park et al., 1999;Tucci et

al., 2001) and an upregulation in neurons in the intact side (Tucci et al., 2001). These findings suggest that the deafferented cochlear nucleus modulates synaptic activity in the intact side, most likely through a commissural inhibitory projection between the contralateral and ipsilateral cochlear nuclei (Cant and Gaston, 1982;Wenthold, 1987;Schofield and Cant, 1996;Alibardi, 1998;Nakamura et al., 2003). This projection arises from multipolar cells that synapse with all the major cell types of the contralateral cochlear nuclei including those that project to the inferior colliculus (Schofield and cant, 1996). Thus, cochlear ablation abolishes activity in the ipsilateral ventral cochlear nucleus, resulting in a decrease in the calretinin-immunostained area within neurons, whereas it disinhibits neurons in the contralateral cochlear nucleus, resulting in activity-dependent increase in the calretinin-immunostained area within those neurons.

Plastic changes in the cochlear nuclei after deafferentation

Early postnatal auditory deprivation leads to other anatomical changes in the cochlear nuclei such as reduction in cell size and volume of the AVCN and PVCN but not in the DCN (Powell and Erulcar, 1962;Coleman and O'Connor, 1979;Conlee and Parks, 1981;Born and Rubel, 1985;Moore and Kowalchuk, 1988;Trune and Morgan, 1988;Moore, 1990;Lesperance et al., 1995;Tierney et al., 1997). Some of these changes can be detected as soon as 24 hours after deafferentation or deprivation (Sie and Rubel, 1992). Previous studies in both gerbils and ferrets suggest that cochlear ablation after the first postnatal week produces cell atrophy without significant cell loss (Tierney et al., 1997;Moore, 1990). In the present study, cochlear ablations were performed in young ferrets just after hearing onset, avoiding the sensitive period around onset of hearing when cell survival is in part dependent on afferent inputs. Similar to the studies mentioned above, cell size and volume are reduced in the AVCN and PVCN but not in the DCN. The fact that this reduction in cell size and volume occurs along with changes in calretinin immunostaining is important for interpretation of our findings. The observation that there is a reduction in AVCN and PVCN volume after cochlear ablation as well as a reduction in calretinin-immunostained neuropil is consistent with the degeneration of calretinin afferent endings from the cochlear nerve, or downregulation of calretinin levels, or both.

In the present study, the decrease in calretinin-immunostained neuropil occurring together with a decreased area of synaptophysin immunostaining, but similar numbers of synaptic endings in the ipsilateral AVCN and PVCN, is consistent with the presence of new, small synapses in place of the previous population of calretinin-immunostained endings. These results are in agreement with previous studies (Illing and Horvath, 1995;Benson et al., 1997) suggesting that a decrease in synaptophysin-immunostained area is due to loss of large primary afferent endings after cochlear ablation that may have been replaced by sprouting of small endings from other intrinsic or descending sources. Degeneration of synaptic endings followed by synaptogenesis has also been reported in the ipsilateral cochlear nucleus after noise exposure that produces cochlear damage (Muly et al., 2002). However, one difference between previous studies and the present findings in unilaterally deafened ferrets is that previously synaptogenesis was detected only in the AVCN whereas the present results suggest that the growth of synaptic endings also occurred in the PVCN. Differences in these findings might be due to species variations or age of the animal when deafferentation was performed.

Correlation of plastic changes in calretinin immunostaining within cochlear nucleus neurons with changes in calretinin immunostaining in axonal endings from cochlear nucleus projection neurons

Previously a dense calretinin-immunostained plexus was described in the dorsolateral part of the central nucleus of the ferret IC, and an increase in immunostaining in the contralateral IC was found after unilateral cochlear ablation (Fuentes-Santamaria et al., 2003). Although the afferent source or sources of the calretinin-immunopositive afferent plexus in the central

nucleus of the IC remain to be fully explored, of the main cell types in the cochlear nuclei that project mainly contralaterally to the IC (Helfert et al., 1991;Schofield and Cant, 1996;Cant and Benson, 2003), only multipolar cells are calretinin immunostained in the ferret cochlear nucleus. Multipolar cells have been identified as calretinin immunopositive in other species as well (Vater and Braun, 1994;Idrizvegovic et al., 2001). Several studies have confirmed that unilateral deafening results in an increase both in the number of cells in the cochlear nucleus on the intact side that project to the ipsilateral IC and in the branching of their axonal projections in the IC (Nordeen et al., 1983;Moore and Kitzes, 1985;Moore et al., 1989). Interestingly, Oliver (1987) demonstrated that the ipsilateral projection from the cochlear nucleus to the IC ends mainly in the low-frequency region of the IC, whereas the contralateral projection ends throughout the entire frequency spectrum of the IC. Thus, multipolar cells projecting to the ipsilateral IC from the intact cochlear nucleus following unilateral cochlear ablation may capture additional synaptic space in the contralateral IC vacated by deprived cochlear nucleus neurons with which they compete and, together with upregulation of calretinin, may contribute to increased immunostaining of the calretinin-immunostained afferent plexus in the central nucleus of the IC contralateral to the cochlear ablation (Fig. 11). Further studies will be required to determine whether the population of multipolar cells in the AVCN and PVCN that projects to the IC on the ipsilateral side, the contralateral side, or both is calretinin immunopositive (Fig. 11). Additionally, the contributions of other sources of calretinin-immunopositive afferent projections to the IC must be taken into account.

CONCLUSIONS

The present results demonstrate a decrease of calretinin immunostaining within neurons in the ipsilateral AVCN and PVCN and suggest a new growth of small synaptic endings in the deafferented ventral cochlear nuclei as a consequence of cochlear removal in young ferrets. Likewise, there is a small increase in calretinin immunostaining within AVCN and PVCN neurons contralaterally. These changes in calretinin immunostaining may be due to decreased activity following deafferentation and thus suggest that changes in calretinin may reflect activity-dependent intracellular events that regulate calcium homeostasis and are integral to adaptive changes in cochlear nucleus neurons and their endings in the superior olivary nuclei and IC after deafening.

ACKNOWLEDGMENTS

The authors thank Georgia Alexander for giving us the ferret tissue to perform the Western blot procedure and also Mary Hillebrand for excellent secretarial assistance.

LITERATURE CITED

Adams JC. Ascending projections to the inferior colliculus. J Comp Neurol 1979;183:519–538. [PubMed: 759446]

Alibardi L. Ultrastructural and immunocytochemical characterization of commissural neurons in the ventral cochlear nucleus of the rat. Ann Anat 1998;180:427–438. [PubMed: 9795693]

Alvarado JC, Fuentes-Santamaria V, Brunso-Bechtold J, Henkel CK. Alterations in calretinin immunostaining in the ferret superior olivary complex after cochlear ablation. J Comp Neurol 2004;470:63–79. [PubMed: 14755526]

Andressen C, Blümcke I, Celio MR. Calcium-binding proteins: selective markers of nerve cells. Cell Tissue Res 1993;271:181–208. [PubMed: 8453652]

Arai R, Winsky L, Arai M, Jacobowitz DM. Immunohistochemical localization of calretinin in the rat hindbrain. J Comp Neurol 1991;310:21–44. [PubMed: 1939729]

Baimbridge KG, Celio MR, Rogers JH. Calcium-binding proteins in the nervous system. Trends Neurosci 1992;15:303–308. [PubMed: 1384200]

Benson CG, Gross JS, Suneja SJ, Potashner SJ. Synaptophysin immunostaining in the cochlear nucleus after unilateral cochlear or ossicular removal. Synapse 1997;25:243–257. [PubMed: 9068122]

Born DE, Rubel EW. Afferent influences on brain stem auditory nuclei of the chicken: neuron number and size following cochlea removal. J Comp Neurol 1985;231:435–445. [PubMed: 3968247]

Brunso-Bechtold JK, Thompson GC, Masterton RB. HRP study of the organization of auditory afferents ascending to the central nucleus of the inferior colliculus in cat. J Comp Neurol 1981;197:05–22.

Caicedo A, D'Aldin C, Puel JL, Eybalin M. Distribution of calcium-binding protein immunoreactivities in the guinea pig auditory brainstem. Anat Embryol (Berl) 1996;194:465–487. [PubMed: 8905014]

Caicedo A, D'Aldin C, Eybalin M, Puel JL. Temporary sensory deprivation changes calcium-binding proteins levels in the auditory brainstem. J Comp Neurol 1997;378:1–15. [PubMed: 9120049]

Cant NB. Identification of cell types in the anteroventral cochlear nucleus that project to the inferior colliculus. Neurosci Lett 1982;32:241–246. [PubMed: 7177487]

Cant NB, Benson CG. Parallel auditory pathways: projection patterns of the different neuronal populations in the dorsal and ventral cochlear nuclei. Brain Res Bull 2003;60:457–474. [PubMed: 12787867]

Cant NB, Casseday JH. Projections from the anteroventral cochlear nucleus to the lateral and medial superior olivary nuclei. J Comp Neurol 1986;247:457–476. [PubMed: 3722446]

Cant NB, Gaston KC. Pathways connecting the right and left cochlear nuclei. J Comp Neurol 1982;212:313–326. [PubMed: 6185548]

Coleman JR, O'Connor P. Effects of monaural and binaural sound deprivation on cell development in the anteroventral cochlear nucleus of rats. Exp Neurol 1979;64:553–566. [PubMed: 467549]

Conlee JW, Parks TN. Age and position-dependent effects of monaural acoustic deprivation in nucleus magnocellularis of the chicken. J Comp Neurol 1981;202:373–384. [PubMed: 7298905]

Correa FM, Guilhaume SS, Saavedra JM. Comparative quantification of rat brain and pituitary angiotensin-converting enzime with autoradiographic and enzimatic methods. Brain Res 1991;545:215–222. [PubMed: 1650274]

Couper Leo JM, Devine AH, Brunjes PC. Focal denervation alters cellular phenotypes and survival in the rat olfactory bulb: a developmental analysis. J Comp Neurol 2000;425:409–421. [PubMed: 10972941]

Coutts AA, Irving AJ, Mackie K, Pertwee RG, Anavi-Goffer S. Localisation of cannabinoid Cb1 receptor immunoreactivity in the guinea pig and rat myenteric plexus. J Comp Neurol 2002;448:410–422. [PubMed: 12115703]

Csaba Z, Simon A, Helboe L, Epelbaum J, Dournaud P. Neurochemical characterization of receptor-expressing cell populations by in vivo agonist-induced internalization: insights from the somatostatin sst2A receptor. J Comp Neurol 2002;454:192–199. [PubMed: 12412143]

Davenport AP, Augood SJ, Lawson DE, Emson PC. The use of quantitative immunocytochemistry (QICC) to measure calbindin DK-28-like immunoreactivity in the rat brain. Cell Mol Biol 1990;36:1–11. [PubMed: 2337909]

Davies KG, Schweitzer JB, Looney MR, Bush AJ, Dohan FC Jr, Hermann BP. Synaptophysin immunohistochemistry densitometry measurement in resected human hippocampus: implication for the etiology of hippocampal sclerosis. Epilepsy Res 1998;32:335–344. [PubMed: 9839773]

Di Cunto F, Imarisio S, Hirsch E, Broccoli V, Bulfone A, Migheli A, Atzori C, Turco E, Triolo R, Dotto GP, Silengo L, Altruda F. Defective neurogenesis in citron kinase knockout mice by altered cytokinesis and massive apoptosis. Neuron 2000;28:115–127. [PubMed: 11086988]

Doucet JR, Ryugo DK. Projections from the ventral cochlear nucleus to the dorsal cochlear nucleus in rats. J Comp Neurol 1997;385:245–264. [PubMed: 9268126]

Druga R, Syka J. Ascending and descending projections to the inferior colliculus in the rat. Physiol Bohemoslov 1984;33:31–42. [PubMed: 6709726]

Dyer MA, Cepko CL. $P57^{kip2}$ regulates progenitor cell proliferation and amacrine interneuron development in the mouse retina. Development 2000;127:3593–3605. [PubMed: 10903183]

Floris A, Dino M, Jacobowitz DM, Mugnaini E. The unipolar brush cells of the rat cerebellar cortex and cochlear nucleus are calretinin-positive: a study by light and electron microscopic immunocytochemistry. Anat Embryol 1994;189:495–520. [PubMed: 7978355]

Forster CR, Illing RB. Plasticity of the auditory brainstem: cochleotomy-induced changes of calbindin-D28K expression in the rat. J.Comp Neurol 2000;416:173–187. [PubMed: 10581464]

Frisina RD, Zettel ML, Kelley PE, Walton JP. Distribution of calbindin D-28k immunostaining in the cochlear nucleus of the young adult chinchilla. Hear Res 1995;85:53–68. [PubMed: 7559179]

Fuentes-Santamaria V, Alvarado JC, Brunso-Bechtold JK, Henkel CK. Upregulation of calretinin immunostaining in the ferret inferior colliculus after cochlear ablation. J Comp Neurol 2003a; 460:585–596. [PubMed: 12717716]

Fuentes-Santamaria V, Alvarado JC, Brunso-Bechtold JK, Henkel CK. Changes in calretinin-immunostaining in the cochlear nuclei in ferrets reared with unilateral cochlear ablation. Assoc Res Otolaryngol Abs 2003b;156:40.

Ghosh A, Greenberg ME. Calcium signaling in neurons: molecular mechanisms and cellular consequences. Science 1995;268:239–247. [PubMed: 7716515]

Helfert, RH.; Snead, CR.; Altschuler, RA. The ascending auditory pathways. In: Altschuler, RA., editor. Neurobiology of hearing: the central auditory system. Raven Press; New York: 1991. p. 1-25.

Henkel CK, Brunso-Bechtold JK. Calcium-binding proteins and GABA reveal spatial segregation of cell types within the developing lateral superior olivary nucleus of the ferret. Microsc Res Tech 1998;41:234–245. [PubMed: 9605341]

Hong-Zhen H, Gao N, Lin Z, Gao C, Liu S, Ren J, Xia Y, Wood JD. P2X(7) receptors in the enteric nervous system of guinea-pig small intestine. J Comp Neurol 2001;440:299–310. [PubMed: 11745625]

Hsu SM, Raine L, Fanger H. Use of avidin-biotin-peroxidase complex (ABC) in immunoperoxidase techniques: a comparison between ABC and unlabeled antibody (PAP) procedures. J Histochem Cytochem 1981;29:577–580. [PubMed: 6166661]

Huang X, Chen S, Tietz E. Immunocytochemical detection of regional protein changes in rat brain sections using computer-assisted image analysis. J Histochem Cytochem 1996;44:981–987. [PubMed: 8773563]

Idrizbegovic E, Canlon B, Bross LS, Willot JF, Bogdanovic N. The total number of neurons and calcium binding protein positive neurons during aging in the cochlear nucleus of CBA/Ca mice: a quantitative study. Hear Res 2001;158:102–115. [PubMed: 11506942]

Illing RB, Horvath M. Re-emergence of GAP-43 in cochlear nucleus and superior olive following cochlear ablation in the rat. Neurosci Lett 1995;194:9–12. [PubMed: 7478222]

Illing RB, Kraus KS, Michler SA. Plasticity of the superior olivary complex. Microsc Res Tech 2000;51:364–381. [PubMed: 11071720]

Kadish I, Van Groen T. Low levels of estrogen significantly diminish axonal sprouting after entorhinal cortex lesions in the mouse. J Neurosci 2002;22:4095–4102. [PubMed: 12019328]

Kadish I, Van Groen T. Differences in lesion-induced hippocampal plasticity between mice and rats. Neuroscience 2003;116:499–509. [PubMed: 12559105]

Kadish I, Pradier L, van Groen T. Transgenic mice expressing the human presenilin 1 gene demonstrate enhanced hippocampal reorganization following entorhinal cortex lesions. Brain Res Bull 2002;57:587–594. [PubMed: 11927360]

Kane ESC. Octopus cells in the cochlear nucleus of the cat: heterotypic synapses upon homeotypic neurons. Int J Neurosci 1973;5:251–279. [PubMed: 4132388]

Kane ES. Synaptic organization in the dorsal cochlear nucleus of the cat: a light and electron microscopic study. J Comp Neurol 1974;155:301–330. [PubMed: 4836032]

Kawai Y, Senba E. Spontaneous synaptogenesis in ex vivo sympathetic ganglion and the blockade by serum treatment. J Comp Neurol 2000;424:670–678. [PubMed: 10931488]

Kawasaki T, Nishio T, Kurosawa H, Roder J, Jeromin A. Spatiotemporal distribution of neuronal calcium sensor-1 in the developing rat spinal cord. J Comp Neurol 2003;460:465–475. [PubMed: 12717707]

Khan I, Osaka H, Stanislaus S, Calvo RM, Deerinck T, Yaksh TL, Taylor P. Nicotinic acetylcholine receptor distribution in relation to spinal neurotransmission pathways. J Comp Neurol 2003;467:44–59. [PubMed: 14574679]

Korada S, Schwarts IR. Calcium binding proteins and AMPA glutamate receptor subunits in gerbil cochlear nucleus. Hear Res 2000;140:23–37. [PubMed: 10675633]

Kubke MF, Gauger B, Basu L, Wagner H, Carr CE. Development of calretinin immunostaining in the brainstem auditory nuclei of the barn owl (*Tyto alba*). J Comp Neurol 1999;415:189–203. [PubMed: 10545159]

Lee EJ, Kim HJ, Lim EJ, Kim IB, Kang WS, Oh SJ, Rickman DW, Chung JW, Chun MH. AII amacrine cells in the mammalian retina show disabled-1 immunoreactivity. J Comp Neurol 2004;470:372–381. [PubMed: 14961563]

Lesperance MM, Helfert RH, Altschuler RA. Deafness induced cell size changes in rostral AVCN of the guinea pig. Hear Res 1995;86:77–81. [PubMed: 8567424]

Li S, Reinprecht I, Fahnestock M, Racine RJ. Activity-dependent changes in synaptophysin immunoreactivity in hippocampus, piriform cortex, and entorhinal cortex of the rat. Neuroscience 2002;115:1221–1229. [PubMed: 12453493]

Lim JH, Brunjes PC. Calcium-binding proteins: differential expression in the rat olfactory cortex after neonatal olfactory bulbectomy. J Neurobiol 1999;39:207–217. [PubMed: 10235675]

Lin L-H, Talman WT. N-methyl-d-aspartate receptor on neurons that synthesize nitric oxide in rat nucleus tractus solitarii. Neuroscience 2000;100:581–588. [PubMed: 11098121]

Lohman C, Friauf E. Distribution of the calcium-binding proteins parvalbumin and calretinin in the auditory brainstem of adult and developing rats. J Comp Neurol 1996;367:90–109. [PubMed: 8867285]

Luo L, Ryan AF, Saint Marie RL. Cochlear ablation alters acoustically induced c-fos mRNA expression in the adult rat auditory brainstem. J Comp Neurol 1999;404:271–283. [PubMed: 9934999]

Masliah E, Terry RD, Alford M, DeTeresa R. Quantitative immunohistochemistry of synaptophysin in human neocortex: an alternative method to estimate density of presynaptic terminals in paraffin sections. J Histochem Cytochem 1990;38:837–844. [PubMed: 2110586]

Masliah E, Fagan AM, Terry RD, DeTeresa R, Mallory M, Gage FH. Reactive synaptogenesis assessed by synaptophysin immunoreactivity is associated with GAP-43 in the dentate gyrus of the adult rat. Exp Neurol 1991;113:131–142. [PubMed: 1831150]

Masliah E, Rockenstein E, Veinbergs I, Sagara Y, Mallory M, Hashimoto M, Mucke L. Beta-amyloid peptides enhance alpha-synuclein accumulation and neuronal deficits in a transgenic mouse model linking Alzheimer's disease and Parkinson's disease. Proc Natl Acad Sci U S A 2001;98:12245–12250. [PubMed: 11572944]

Miller RJ. Regulation of calcium homoeostasis in neurons: the role of calcium-binding proteins. Biochem Soc Trans 1995;23:629–632. [PubMed: 8566431]

Mirich JM, Williams NC, Berlau DJ, Brunjes PC. Comparative study of aging in the mouse olfactory bulb. J Comp Neurol 2002;454:361–372. [PubMed: 12455003]

Moore DR. Auditory brainstem of the ferrets: sources of projections to the inferior colliculus. J Comp Neurol 1988;269:342–354. [PubMed: 2453533]

Moore DR. Auditory brainstem of the ferret: early cessation of developmental sensitivity of neurons in the cochlear nucleus to removal of the cochlea. J Comp Neurol 1990;302:810–823. [PubMed: 2081818]

Moore DR, Kitzes LM. Projections from the cochlear nucleus to the inferior colliculus in normal and neonatally cochlea-ablated gerbils. J Comp Neurol 1985;240:180–195. [PubMed: 4056109]

Moore DR, Kowalchuk NE. An anomaly in the auditory brain stem projections of hypopigmented ferrets. Hear Res 1988;35:275–278. [PubMed: 3198516]

Moore DR, Hutchings ME, King AJ, Kowalchuk NE. Auditory brainstem of the ferret: some effects of rearing with a unilateral earplug on the cochlea, cochlear nucleus, and projections to the inferior colliculus. J Neurosci 1989;9:1213–1222. [PubMed: 2539441]

Mostafapour SP, Cochran SL, Del Puerto NM, Rubel EW. Patterns of cell death in mouse anteroventral cochlear nucleus neurons after unilateral cochlea removal. J Comp Neurol 2000;426:561–571. [PubMed: 11027399]

Muly SM, Gross JS, Morest DK, Potashner SJ. Synaptophysin in the cochlear nucleus following acoustic trauma. Exp Neurol 2002;177:202–221. [PubMed: 12429223]

Nakamura M, Rosahl SK, Alkahlout E, Gharabaghi A, Walter GF, Sam M. C-Fos immunoreactivity mapping of the auditory system after electrical stimulation of the cochlear nerve in rats. Hear Res 2003;184:75–81. [PubMed: 14553905]

Nordeen KW, Killackey HP, Kitzes LM. Ascending projections to the inferior colliculus following unilateral cochlear ablation in the neonatal gerbil, *Meriones unguiculatus*. J Comp Neurol 1983;214:144–153. [PubMed: 6841682]

Nunzi MG, Birnstiel S, Bhattacharyya BJ, Slater NT, Mugnaini E. Unipolar brush cells form a glutamatergic projection system within the mouse cerebellar cortex. J Comp Neurol 2001;434:329–341. [PubMed: 11331532]

O'Donnell AM, Ellis LM, Riedl MS, Elde RP, Mawe GM. Distribution and chemical coding of orphanin FQ/nociceptin-immunoreactive neurons in the myenteric plexus of guinea pig intestines and sphincter of Oddi. J Comp Neurol 2001;430:1–11. [PubMed: 11135242]

Oliver DL. Projections to the inferior colliculus from the anteroventral cochlear nucleus in the cat: possible substrates for binaural interactions. J Comp Neurol 1987;264:24–46. [PubMed: 2445792]

Oliver DL, Morest DK. The central nucleus of the inferior colliculus in the cat. J Comp Neurol 1984;222:237–264. [PubMed: 6699209]

Osen KK. Cytoarchitecture of the cochlear nuclei in the cat. J Comp Neurol 1969;136:453–484. [PubMed: 5801446]

Park DL, Girod DA, Durham D. Tonotopic changes in 2-deoxyglucose activity in chick cochlear nucleus during hair cell loss and regeneration. Hear Res 1999;138:45–55. [PubMed: 10575113]

Parks TN, Code RA, Taylor DA, Solum DA, Strauss DM, Jacobowitz DM. Calretinin expression in the chick brainstem auditory nuclei develops and is maintained independently of cochlear nerve input. J Comp Neurol 1997;383:112–121. [PubMed: 9184990]

Peretti-Renucci R, Feuerstein C, Manier M, Lorimier P, Sabasta M, Thibault J, Mons N, Geffard M. Quantitative image analysis with densitometry for immunohistochemistry and autoradiography of receptor binding sites-methodological considerations. J Neurosci Res 1991;28:583–600. [PubMed: 1678436]

Philpot BD, Lim JH, Brunjes PC. Activity-dependent regulation of calcium-binding proteins in the developing rat olfactory bulb. J Comp Neurol 1997;387:12–26. [PubMed: 9331168]

Potashner SJ, Suneja SK, Benson CG. Regulation of D-aspartate release and uptake in adult brain stem auditory nuclei after unilateral middle ossicle removal and cochlear ablation. Exp Neurol 1997;148:222–235. [PubMed: 9398464]

Powell TP, Erulkar SD. Transneuronal cell degeneration in the auditory relay nuclei of the cat. J Anat (Lond) 1962;96:249–268. [PubMed: 14488390]

Resibois A, Rogers JH. Calretinin in rat brain: an immunohistochemical study. Neuroscience 1992;46:101–134. [PubMed: 1594096]

Rogers JH. Two calcium-binding proteins mark many chick sensory neurons. Neuroscience 1989;31:697–709. [PubMed: 2594198]

Ryugo DK, Parks TN. Primary innervation of the avian and mammalian cochlear nucleus. Brain Res Bull 2003;60:435–456. [PubMed: 12787866]

Ryugo DK, Willard FH. The dorsal cochlear nucleus of the mouse: a light microscopic analysis of neurons that project to the inferior colliculus. J Comp Neurol 1985;242:381–36. [PubMed: 2418077]

Schofield BR, Cant NB. Projections from the ventral cochlear nucleus to the inferior colliculus and the contralateral cochlear nucleus in guinea pigs. Hear Res 1996;102:1–14. [PubMed: 8951445]

Shneiderman A, Henkel CK. Evidence of collateral axonal projections to the superior olivary complex. Hear Res 1985;19:199–205. [PubMed: 2999051]

Shneiderman A, Henkel CK. Banding of lateral superior olivary nucleus afferents in the inferior colliculus: a possible substrate for sensory integration. J Comp Neurol 1987;266:519–534. [PubMed: 2449472]

Sie KC, Rubel EW. Rapid changes in protein synthesis and cell size in the cochlear nucleus following eighth nerve activity blockade or cochlea ablation. J Comp Neurol 1992;320:501–508. [PubMed: 1629400]

Stack KE, Code RA. Calretinin expression in the chick cochlear nucleus after deafferentation. Brain Res 2000;873:135–139. [PubMed: 10915820]

Stroemer RP, Kent TA, Hulsebosch CE. Enhanced neocortical neural sprouting, synaptogenesis, and behavioral recovery with D-amphetamine therapy after neocortical infarction in rats. Stroke 1998;29:2381–2393. [PubMed: 9804653]

Syka J. Plastic changes in the central auditory system after hearing loss, restoration of function, and during learning. Physiol Rev 2002;82:601–636. [PubMed: 12087130]

Tierney TS, Russel FA, Moore DR. Susceptibility of developing cochlear nucleus neurons to deafferentation-induced death abruptly ends just before the onset of hearing. J Comp Neurol 1997;378:295–306. [PubMed: 9120067]

Trune DR, Morgan CR. Stimulation-dependent development of neuronal cytoplasm in mouse cochlear nucleus. Hear Res 1988;33:141–150. [PubMed: 3397324]

Tucci DL, Cant NB, Durham D. Effects of conductive hearing loss on gerbil central auditory system activity in silence. Hear Res 2001;155:124–132. [PubMed: 11335082]

Vater M, Braun K. Parvalbumin, calbindin D-28K, and calretinin immunostaining in the ascending auditory pathway of horseshoe bats. J Comp Neurol 1994;341:534–558. [PubMed: 8201027]

Wenthold RJ. Evidence for a glycinergic pathway connecting the two cochlear nuclei: an immunocytochemical and retrograde transport study. Brain Res 1987;415:183–187. [PubMed: 3304530]

Winsky L, Jacobowitz DM. Effects of unilateral cochlea ablation on the distribution of calretinin mRNA and immunostaining in the guinea pig ventral cochlear nucleus. J Comp Neurol 1995;354:564–582. [PubMed: 7608338]

Yao W, Godfrey DA. Densitometric evaluation of markers for cholinergic transmission in rat superior olivary complex. Neurosci Lett 229:21–24. [PubMed: 9224792]197

Zettel ML, Carr CE, O'Neill WE. Calbindin-like immunostaining in the central auditory system of the mustached bat, *Pteronotus parnellii*. J Comp Neurol 1991;313:1–16. [PubMed: 1761747]

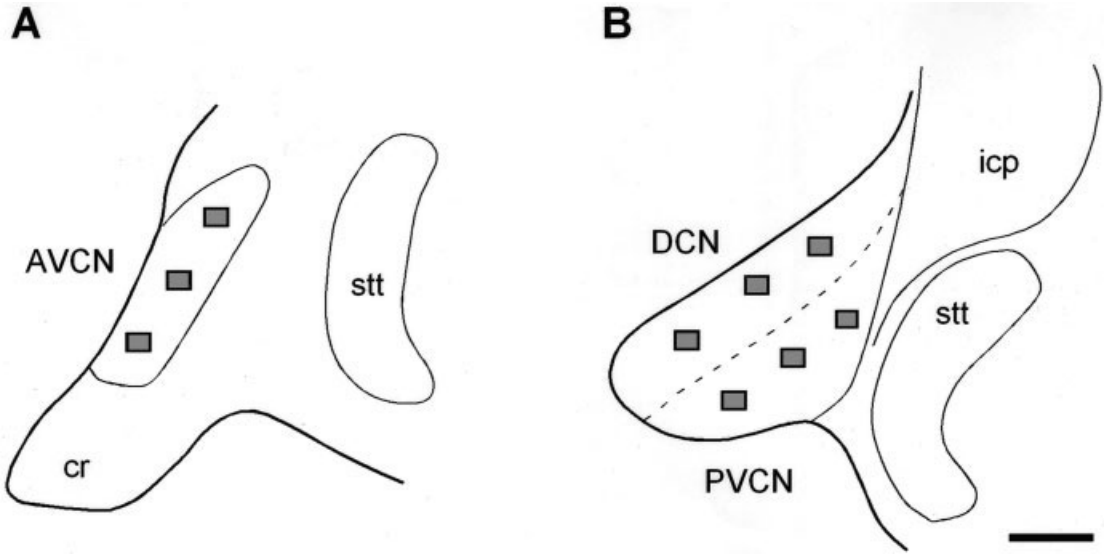

Fig 1.

A,B: Line drawings showing samples of selected fields for quantification of synaptophysin immunostaining in the AVCN, PVCN and DCN in control and ablated animals. AVCN, anterior ventral cochlear nucleus; cr, cochlear root; DCN, dorsal cochlear nucleus; icp, inferior cerebellar peduncle; PVCN, posterior ventral cochlear nucleus; stt, spinal trigeminal tract. Scale bar = 500 μm in B (applies to A,B).

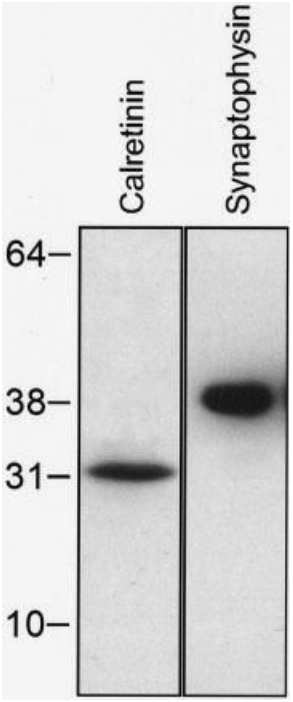

Fig 2.

Western blot showing detection of calretinin and synaptophysin antibodies in the ferret cochlear nucleus. Positions of molecular weight markers (kDa) are indicated in the left side. Immunoreactive single bands were detected at 31kDa and 38kDa for calretinin and synaptophysin, respectively.

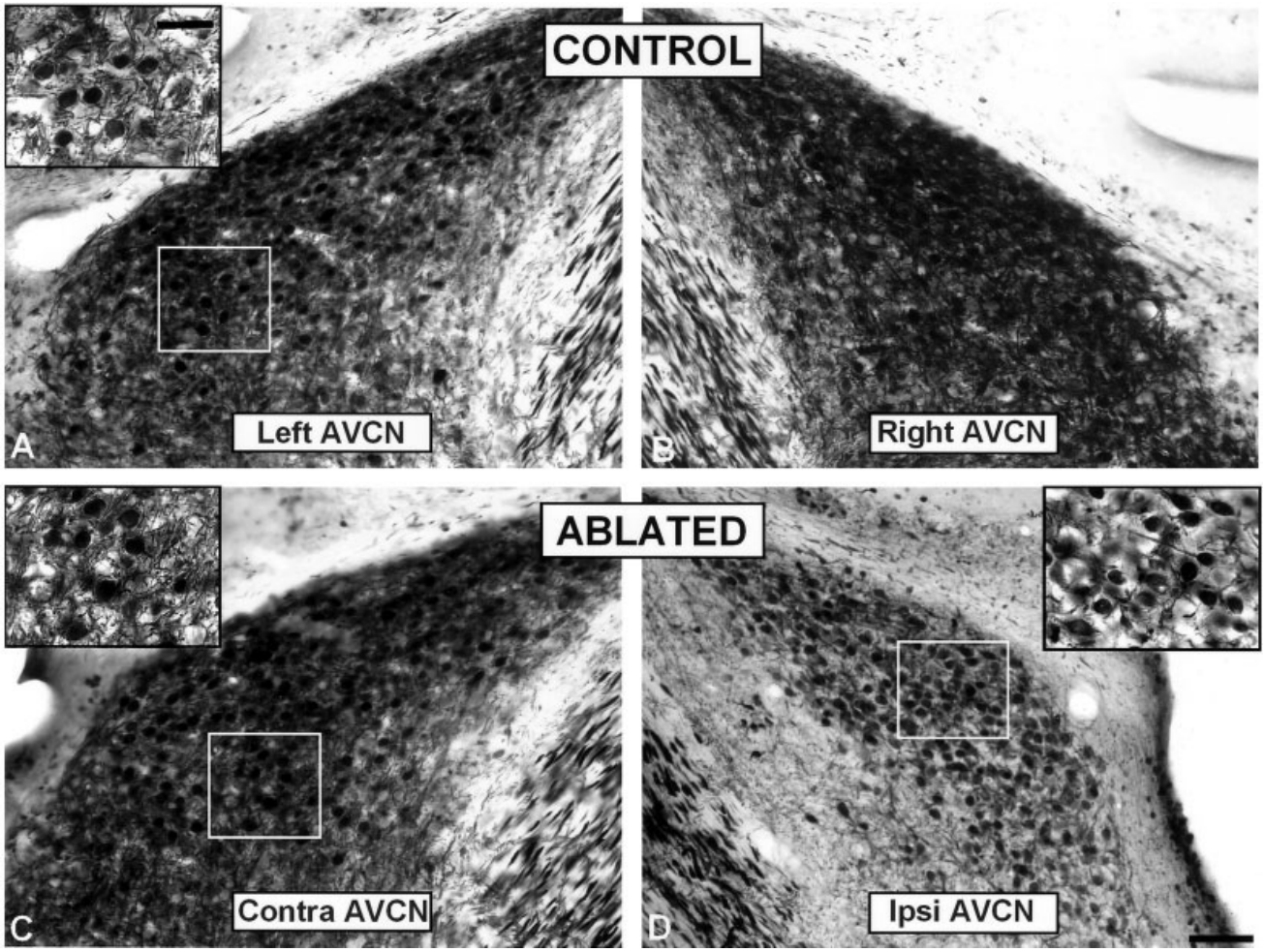

Fig 3.

Digital images illustrating calretinin immunostaining in the AVCN in control (**A,B**) and ablated ferrets (**C,D**). Immunostaining in the neuropil was decreased in the ipsilateral AVCN (see inset in D) compared to the contralateral side (see inset in C) and unoperated animals (see inset in A). AVCN, anterior ventral cochlear nucleus. Scale bars = 250 μm in D (applies to A–D); 50 μm in inset A (applies to inset A,C,D).

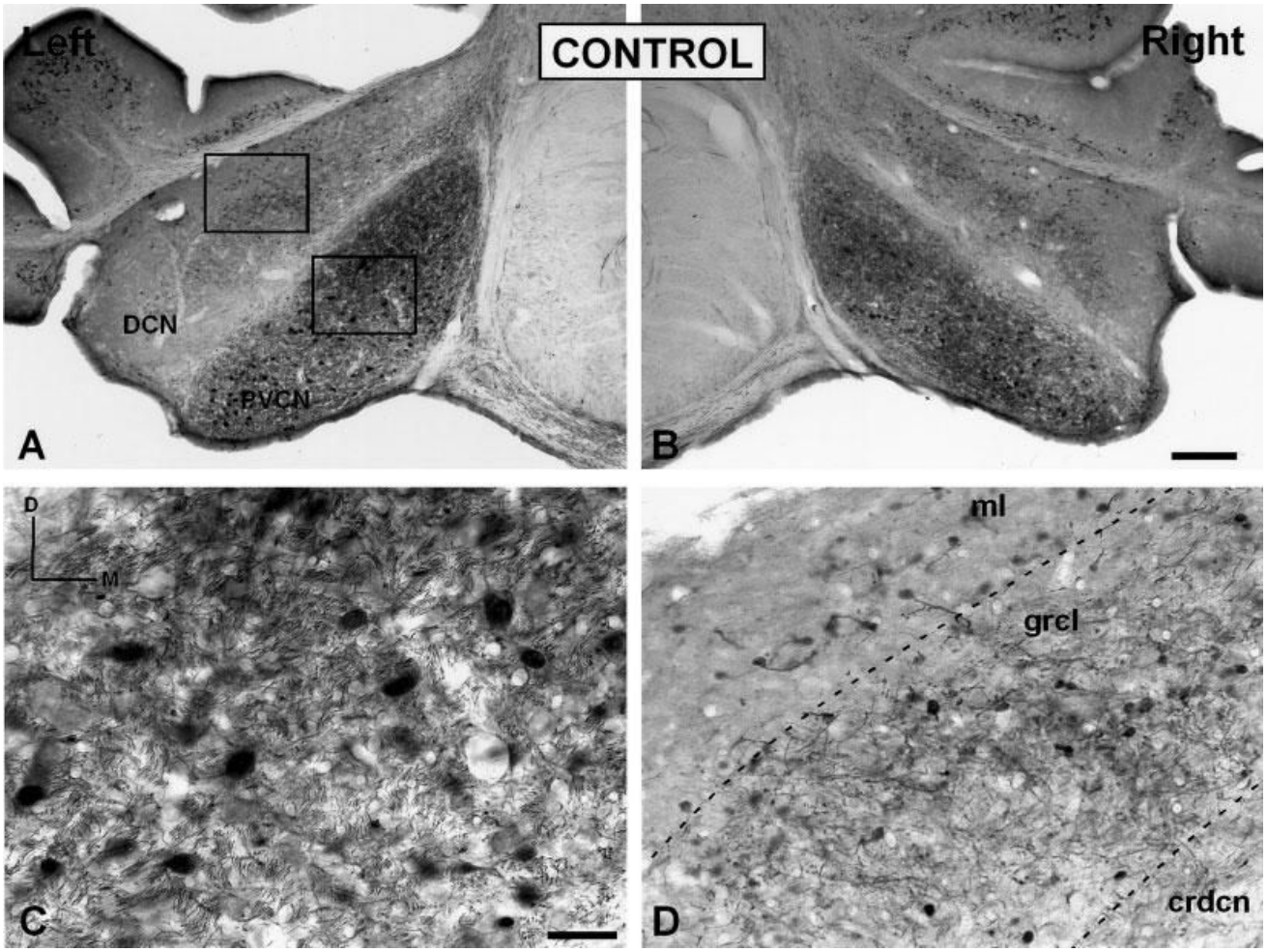

Fig 4.

Low- (**A,B**) and high- (**C,D**) magnification digital images illustrating calretinin immunostaining in the PVCN and DCN in control ferrets. In the PVCN, a dense calretinin immunostained neuropil and immunostained cells were evident throughout the nucleus (C). In the DCN, calretinin immunostained neurons were more abundant in the granular cell layer than in the molecular and central region of the DCN (D). AVCN, anterior ventral cochlear nucleus; crdcn, central region of the DCN; DCN, dorsal cochlear nucleus; grcl, granular cell layer; ml, molecular layer; PVCN, posterior ventral cochlear nucleus. Scale bars = 100 μm in B (applies to A,B); 50 μmin C (applies to C,D).

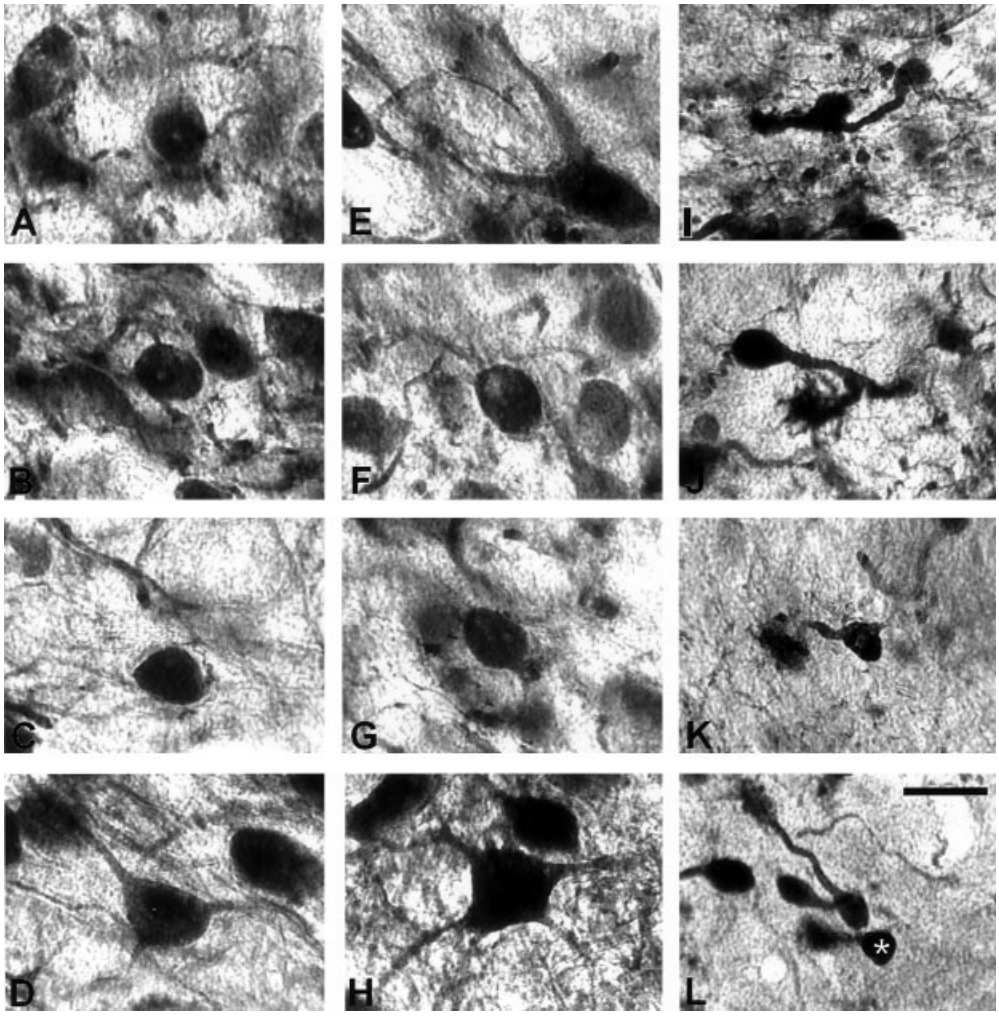

Fig 5.

High-magnification digital images showing calretinin immunostained cells in the cochlear nuclei in control ferrets. Immunostained spherical cells (**A,B**), globular cells (**C**) and multipolar cells (**D**) in the anterior ventral cochlear nucleus, octopus cells (**E**), globular cells (**F,G**) and multipolar cells (**H**) in the posterior ventral cochlear nucleus and granular cells (**I,J**) and unipolar brush cells (**K,L**; white asterisk) in the dorsal cochlear nucleus were identified in these cases. Scale bar = 25 μm in L (applies to A–L).

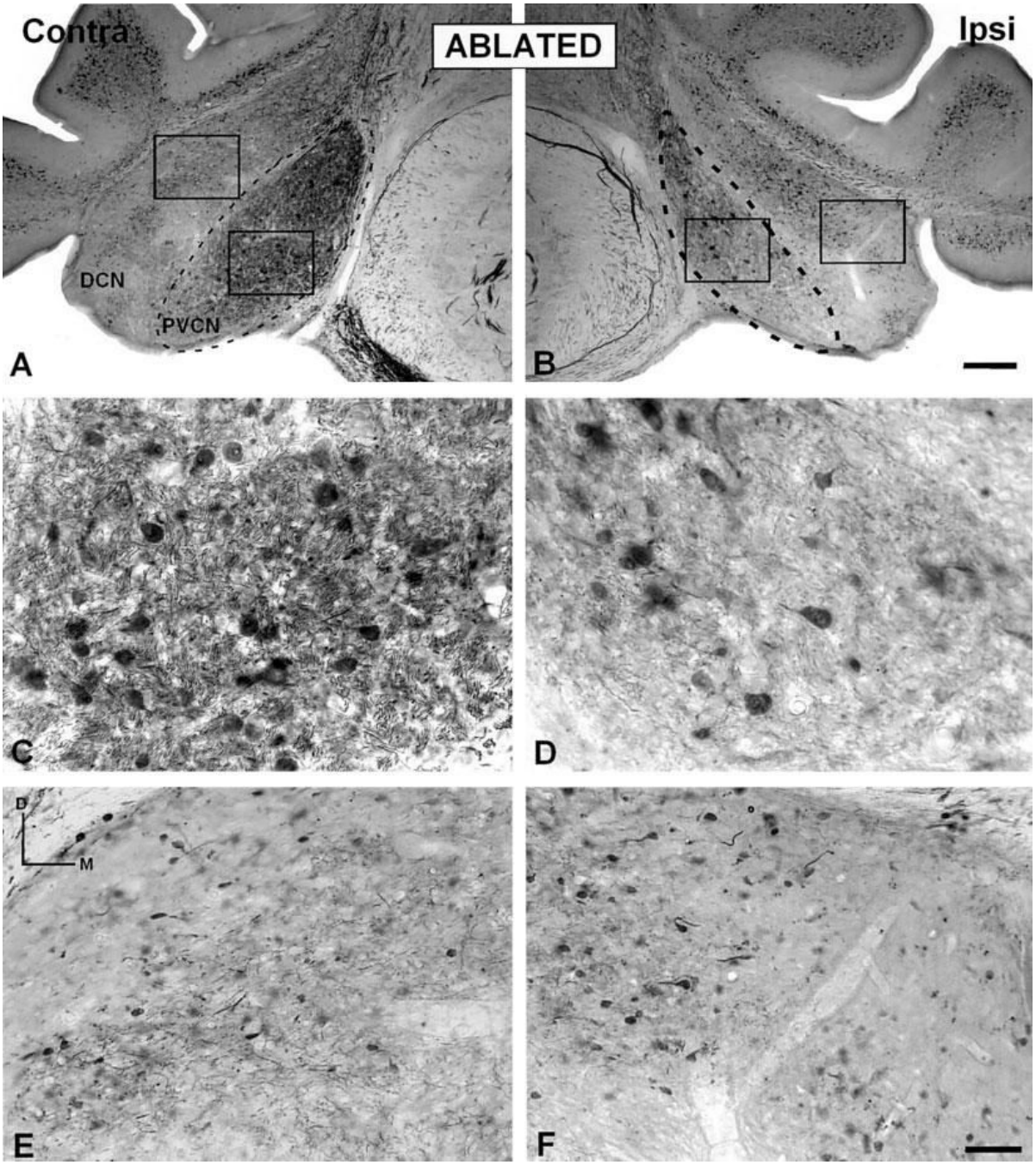

Fig 6.

A–F: Digital images illustrating calretinin immunostaining in the PVCN and DCN in ablated ferrets. A decreased calretinin immunostained neuropil was evident in the ipsilateral PVCN (D) compared to the contralateral side (C) and unoperated animals (see, Fig. 3C). However, no differences were found in either the ipsilateral DCN (F) or the DCN on the intact side (E). AVCN, anterior ventral cochlear nucleus; contra, contralateral; DCN, dorsal cochlear nucleus; ipsi, ipsilateral; PVCN, posterior ventral cochlear nucleus. Scale bars = 100 μm in B (applies to A,B); 50 μm in F (applies to C–F).

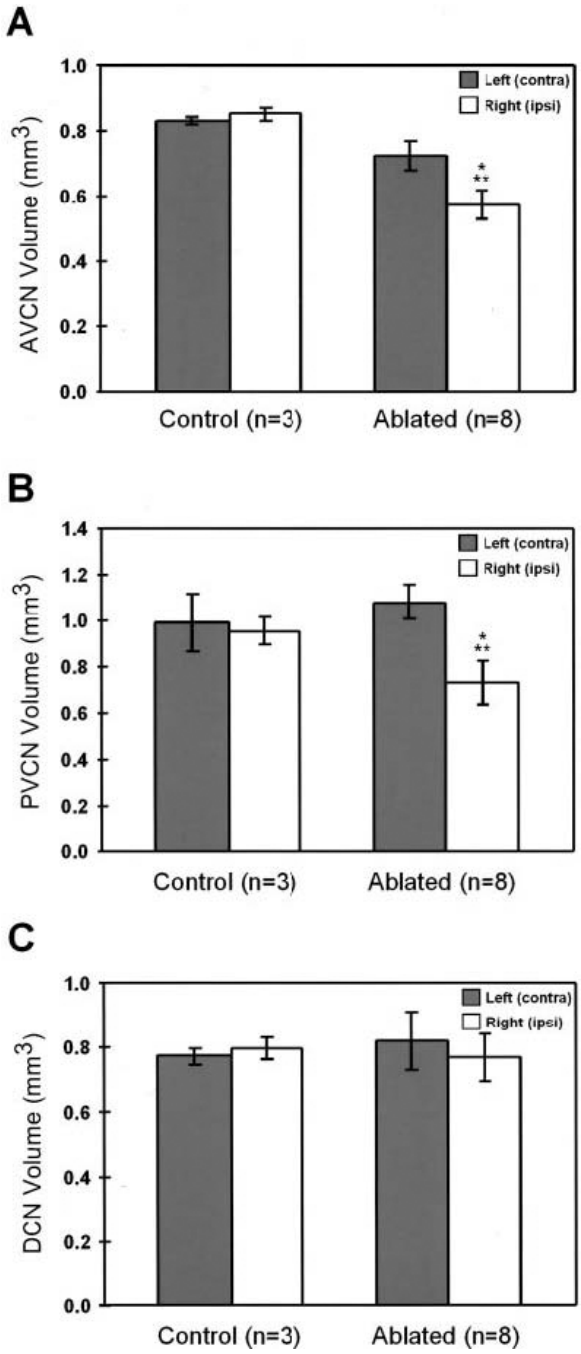

Fig 7.

Bar graphs showing the mean volume of the left and right anterior ventral cochlear nucleus (AVCN), posterior ventral cochlear nucleus (PVCN) and dorsal cochlear nucleus (DCN), in control and ablated ferrets. There was a significant decrease in the AVCN (**A**) and PVCN (**B**) volume ipsilateral to the ablation compared to both the contralateral side and unoperated animals. However, no significant differences were found in the DCN (**C**) either between sides or animal groups. Error bars indicate standard deviation. (*), indicates significant differences between sides ($P<0.05$); (**), indicates significant differences between groups ($P<0.05$).

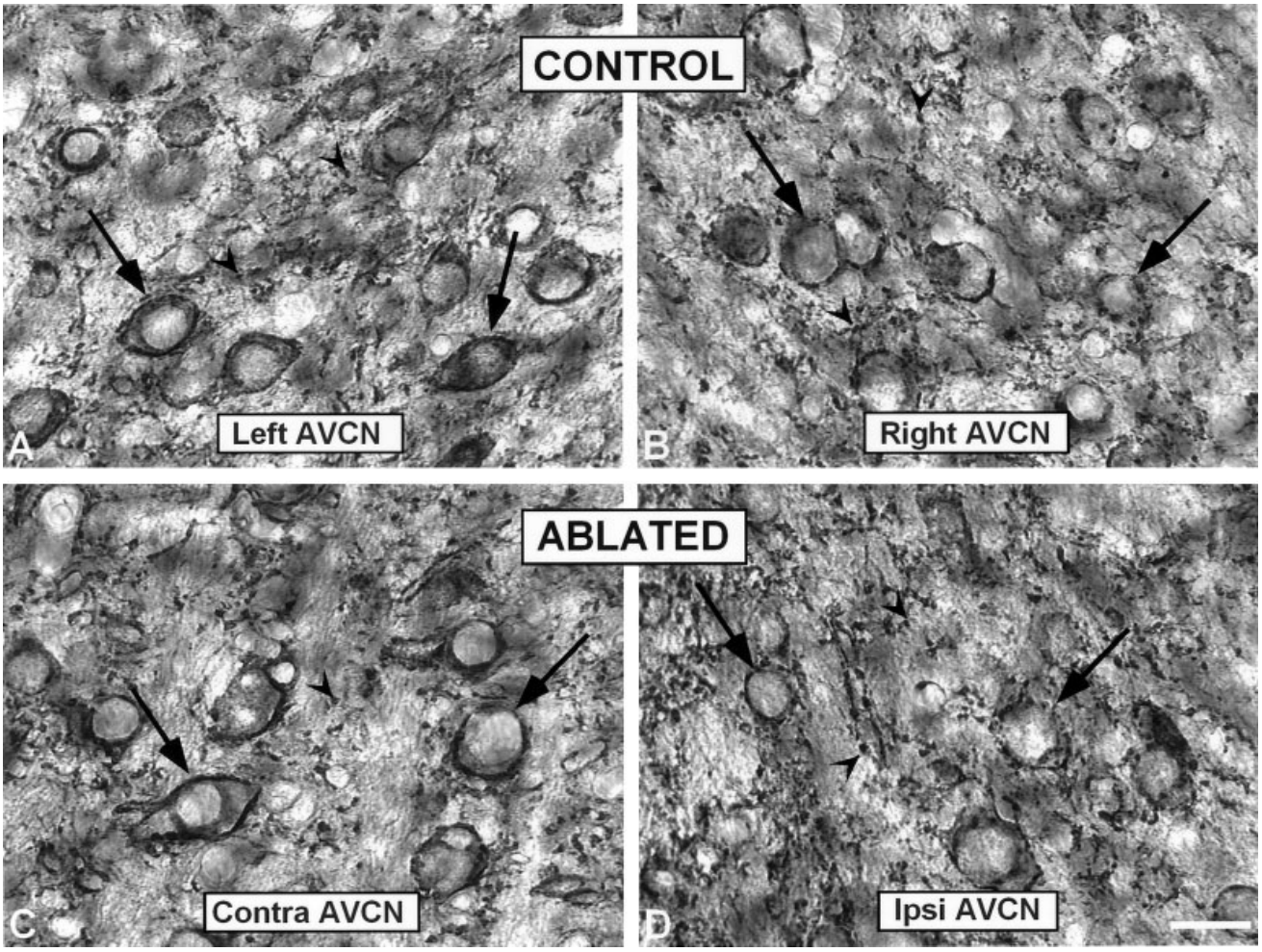

Fig 8.

High-magnification digital images showing synaptophysin immunostaining in the AVCN in control (**A,B**) and ablated (**C,D**) animals. Perisomatic profiles surrounding neurons (arrows) were more frequent than immunopositive boutons (arrowheads) in both control and contralateral side in ablated animals (C). In the ipsilateral side (D) an increase in the number of small immunopositive boutons was evident qualitatively. AVCN, anterior ventral cochlear nucleus; contra, contralateral; ipsi, ipsilateral. Scale bar = 25 μm in D (applies to A–D).

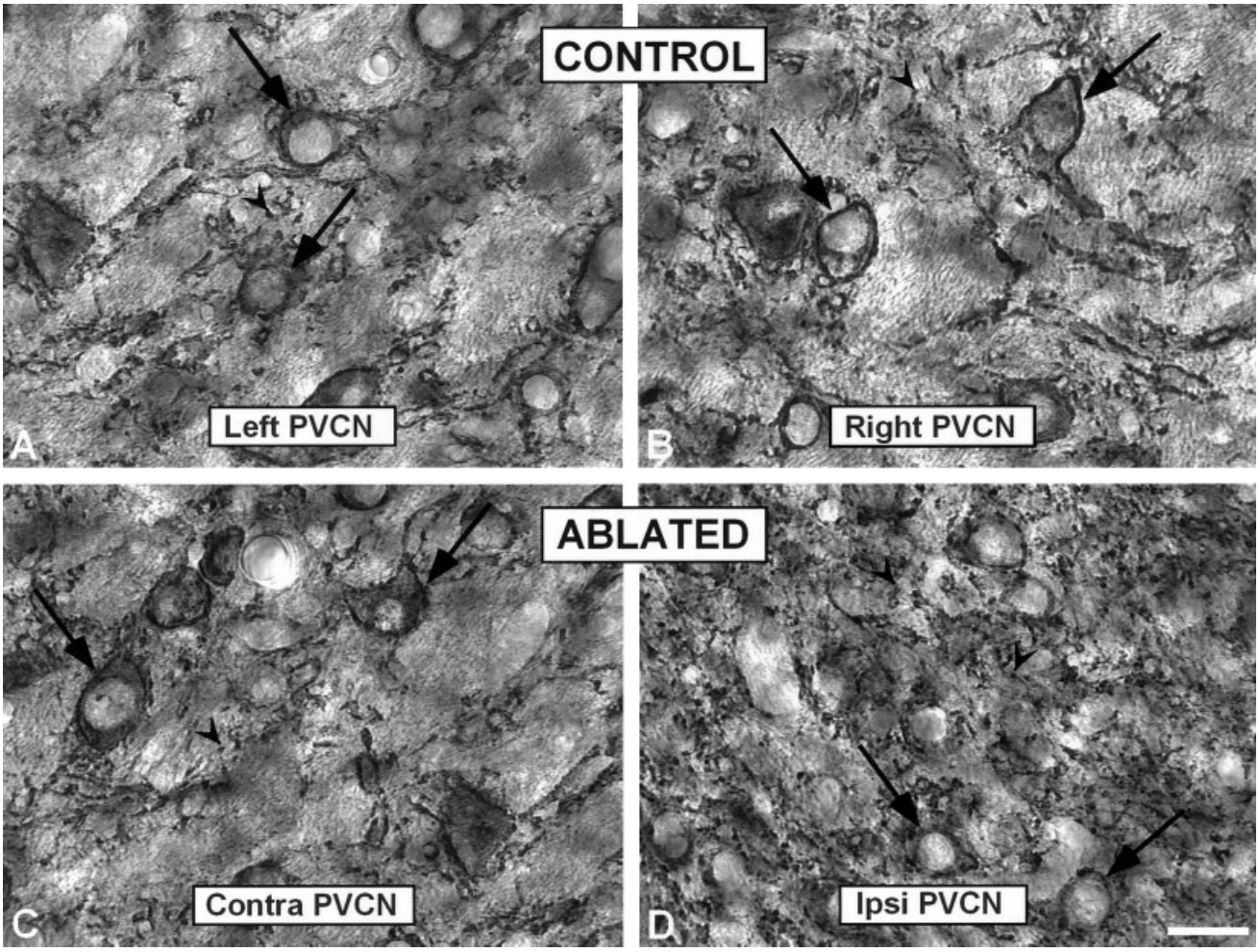

Fig 9.

High-magnification digital images showing synaptophysin immunostaining in the PVCN in control (**A,B**) and ablated (**C,D**) animals. Similar to the anterior ventral cochlear nucleus, large profiles surrounding cell bodies (arrows) were abundant in the PVCN in control and contralateral side in ablated ferrets. In addition, there was a qualitative increase in the number of punctate profiles (arrowheads) in the ipsilateral PVCN (D) compared to the contralateral side (C) and unoperated animals (A,B). PVCN, posterior ventral cochlear nucleus; contra, contralateral; ipsi, ipsilateral. Scale bar = 25 μm in (applies to A–D).

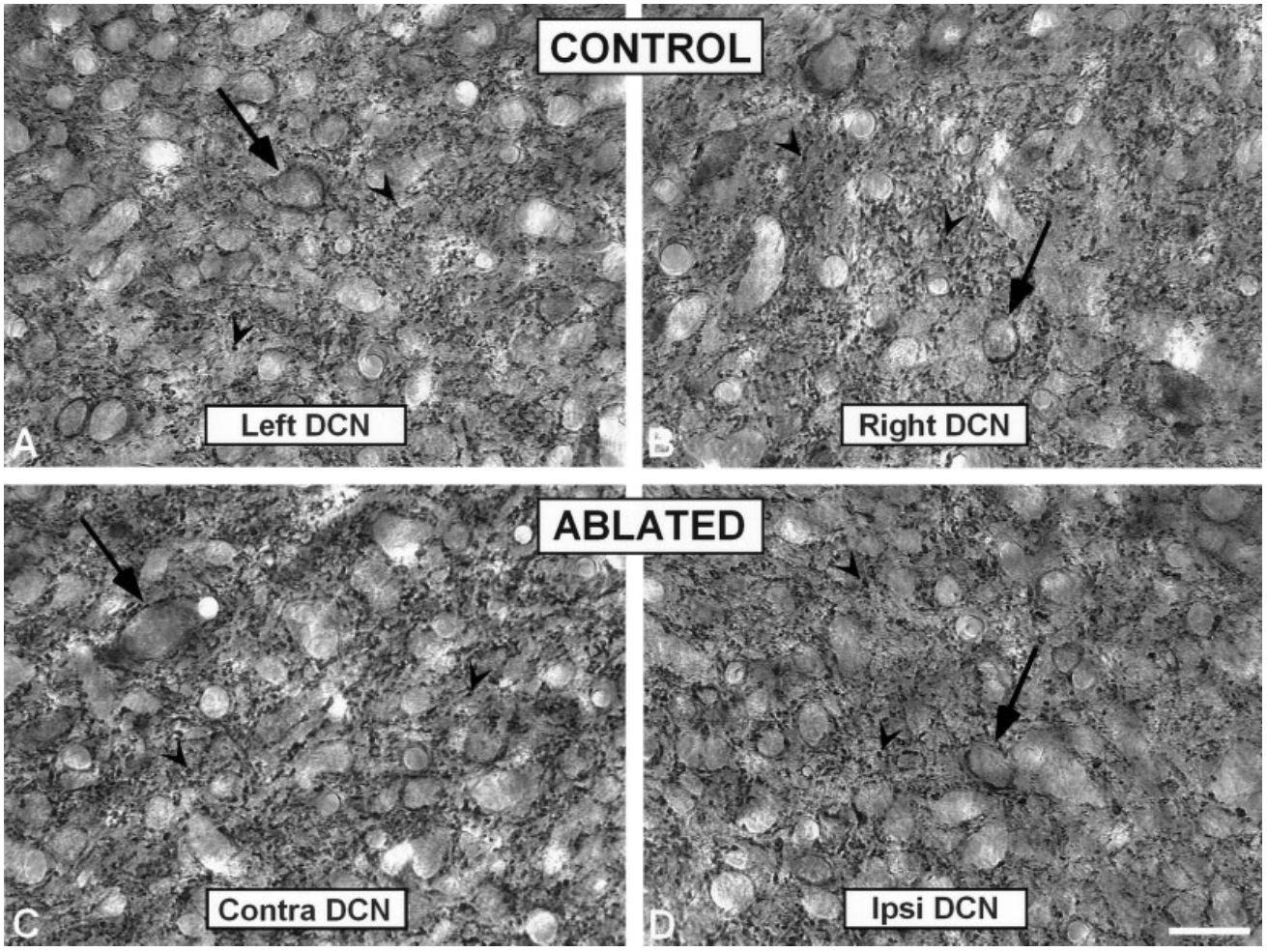

Fig 10.

High-magnification digital images showing synaptophysin immunostaining in the DCN in control (**A,B**) and ablated (**C,D**) animals. Punctate deposits in the neuropil (arrowheads) were frequent throughout the DCN although immunopositive profiles surrounding unstained somata (arrows) were also present. No increases in synaptophysin immunopositive profiles were found. contra, contralateral; DCN, dorsal cochlear nucleus; ipsi, ipsilateral. Scale bar = 25 μm in D (applies to A–D).

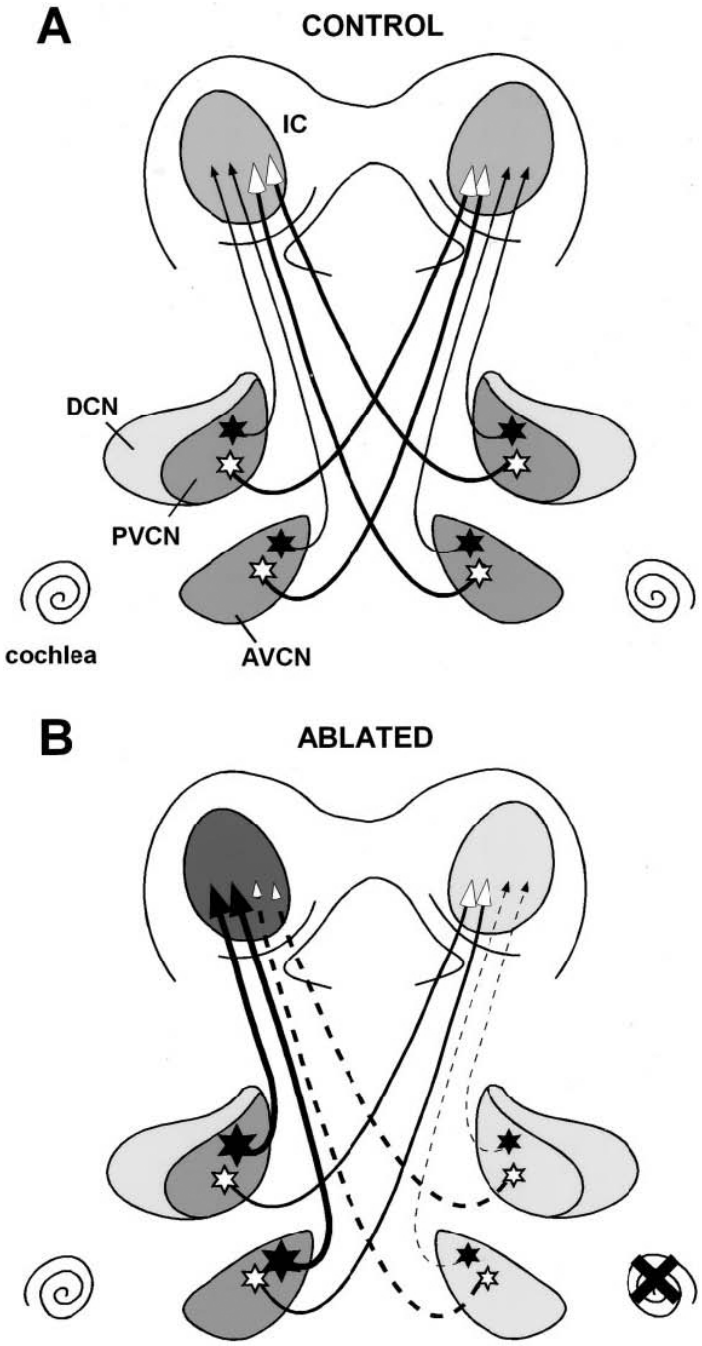

Fig 11.

Schematic representation of calretinin immunostaining in the young adult ferret cochlear nucleus and IC following cochlear ablation at hearing onset. In control animals (**A**), multipolar neurons (stars) in anterior ventral cochlear nucleus and posterior ventral cochlear nucleus project bilaterally although calretinin immunostained neurons project predominantly to the ipsilateral IC. In cochlear ablation (**B**), upregulation of calretinin in multipolar cells in the intact cochlear nuclei contributes to increased immunostaining in the calretinin plexus in the IC on the side contralateral to the ablation. Conversely, downregulation of calretinin in multipolar cells in the deprived cochlear nucleus contributes to reduce immunostaining plexus of the IC on the side ipsilateral to the ablation. Dashed lines represent deprived projections while solid

lines intact projections. Calretinin immunostained cells are indicated with solid stars and calretinin immunonegative cells with open stars. Different gray colors indicate different levels of immunostained neuropil or fibers in each nucleus. Accordingly, darker gray color indicates an upregulation and lighter gray color a downregulation in calretinin immunostaining. AVCN, anterior ventral cochlear nucleus; DCN, dorsal cochlear nucleus; IC, inferior colliculus; PVCN, posterior ventral cochlear nucleus.

TABLE 1

Calretinin Immunostaining in AVCN, PVCN, and DCN in Control (N = 3) and Ablated (N = 8) Animals[1]

	Left side (contralateral)			Right side (ipsilateral)		
	Nucleus mean gray level	**Mean gray level within neurons**	**Neuron immunostained area (μm²)**	**Nucleus mean gray level**	**Mean gray level within neurons**	**Neuron immunostained area (μm²)**
Control						
AVCN	1.62 ± 0.07	1.76 ± 0.06	171.39 ± 6.56(**)	1.62 ± 0.04(**)	1.76 ± 0.08	171.58 ± 1.33(**)
PVCN	1.60 ± 0.06	1.74 ± 0.06	177.43 ± 4.51(**)	1.60 ± 0.09(**)	1.76 ± 0.07	176.66 ± 4.53(**)
DCN	1.25 ± 0.06	1.75 ± 0.06	53.85 ± 4.43	1.26 ± 0.05	1.75 ± 0.06	54.98 ± 6.45
Ablated						
AVCN	1.77 ± 0.08(*)	1.80 ± 0.01	184.62 ± 4.54(*)(**)	1.28 ± 0.13(*)(**)	1.83 ± 0.02	146.77 ± 7.39(*)(**)
PVCN	1.65 ± 0.09(*)	1.80 ± 0.01	191.01 ± 7.23(*)(**)	1.03 ± 0.22(*)(**)	1.83 ± 0.02	151.13 ± 8.64(*)(**)
DCN	1.29 ± 0.16	1.79 ± 0.02	57.56 ± 4.79	1.28 ± 0.19	1.80 ± 0.02	54.95 ± 7.15

[1] Values expressed are means and standard deviations.

(*) indicates significant differences between sides

(**) indicates significant differences between groups; AVCN, anteroventral; DCN, dorsal cochlear nucleus; PVCN, posteroventral.

TABLE 2

Synaptophysin Immunostaining in AVCN, PVCN, and DCN in Control (N = 3) and Ablated (N = 8) Animals[1]

	Left side (contralateral)			Right side (ipsilateral)		
	Nucleus mean gray level	**Immunostained area (% relative to the entire field)**	**Mean number of boutons**	**Nucleus mean gray level**	**Immunostained area (% relative to the entire field)**	**Mean number of boutons**
Control						
AVCN	93.50 ± 10.15	3.42 ± 0.58	418.44 ± 17.40	96.99 ± 8.04	3.41 ± 0.46(**)	409.02 ± 26.88(**)
PVCN	86.12 ± 12.26	3.98 ± 0.40	416.31 ± 69.61	88.17 ± 19.56	3.99 ± 0.51(**)	413.75 ± 66.87(**)
DCN	97.01 ± 8.52	4.12 ± 0.17	449.64 ± 30.29	99.43 ± 4.29	4.12 ± 0.31	447.36 ± 26.60
Ablated						
AVCN[2]	96.14 ± 16.37	3.51 ± 0.09(*)	415.93 ± 48.14(*)	92.00 ± 11.84	3.60 ± 0.33	529.02 ± 104.83(*)(**)
[3]					2.28 ± 0.31(*)(**)	354.44 ± 70.23
PVCN[2]	96.37 ± 11.68	3.62 ± 0.59(*)	390.24 ± 49.74(*)	98.79 ± 5.71	3.62 ± 0.12	550.29 ± 65.82(*)(**)
[3]					2.78 ± 0.09(*)(**)	374.00 ± 89.24
DCN	87.78 ± 9.04	4.04 ± 0.45	452.21 ± 22.32	91.07 ± 6.21	3.86 ± 0.15	450.70 ± 2.40

[1] Values expressed are means and standard deviations.

[2] Not corrected values.

[3] Corrected values.

(*) indicates significant differences between sides

(**) indicates significant differences between groups; AVCN, anteroventral; DCN, dorsal cochlear nucleus; PVCN, posteroventral.